Electronic Supplementary Material (ESI) for Dalton Transactions.

Electronic Supporting Information for

Hexaiododiplatinate(II) as a Useful Supramolecular Synthon for Halogen Bond Involving Crystal Engineering

Anastasiya A. Eliseeva,[a] Daniil M. Ivanov,[a] Alexander S. Novikov,[a] Anton V. Rozhkov,[a]
Ilya V. Kornyakov,[b] Alexey Yu. Dubovtsev,[a] Vadim Yu. Kukushkin[a,c]*

[a]*Institute of Chemistry, Saint Petersburg State University, Universitetskaya Nab. 7/9, 199034 Saint Petersburg, Russian Federation*

[b]*Institute of Earth Sciences, Saint Petersburg State University, Universitetskaya Nab. 7/9, 199034 Saint Petersburg, Russian Federation*

[c]*Institute of Macromolecular Compounds, Russian Academy of Sciences, Bolshoii Pr., 31, 199004 Saint Petersburg, Russian Federation*

E-mail: v.kukushkin@spbu.ru

Table of Content

S1. Available data on synthesis of $[Pt_2(\mu\text{-}I)_2I_4]^{2-}$ complexes

The conventional procedure for preparation of the iodine-bridged platinum(II) complexes bearing ammonium or phosphonium cations, viz. $[R_4N]_2[Pt_2(\mu\text{-}I)_2I_4]$ (R = Me,[1] Et,[1–3] *n*-Bu (CSD code: CODHIM),[4] *n*-Pn[5]) and $[R_3PR^1]_2[Pt_2(\mu\text{-}I)_2I_4]$ (R = Ph, R^1 = Ph;[6] R = Ph, R^1 = CH_2Ph[2]), involves precipitation of the *in situ* generated $[Pt_2(\mu\text{-}I)_2I_4]^{2-}$ complex from aqueous solutions either $K_2[PtCl_4]$,[2,4,5,7] or PtI_2[1,3,6,8] upon their treatment with excess of KI, followed by slow addition of saturated aqueous solutions of $[R_4N]X$ or $[R_3PR^1]X$ (X = Cl, I), respectively (Fig. S1a). The reaction and crystallization conditions vary depending on the cation used, albeit the synthetic procedure is basically the same in all reported cases.

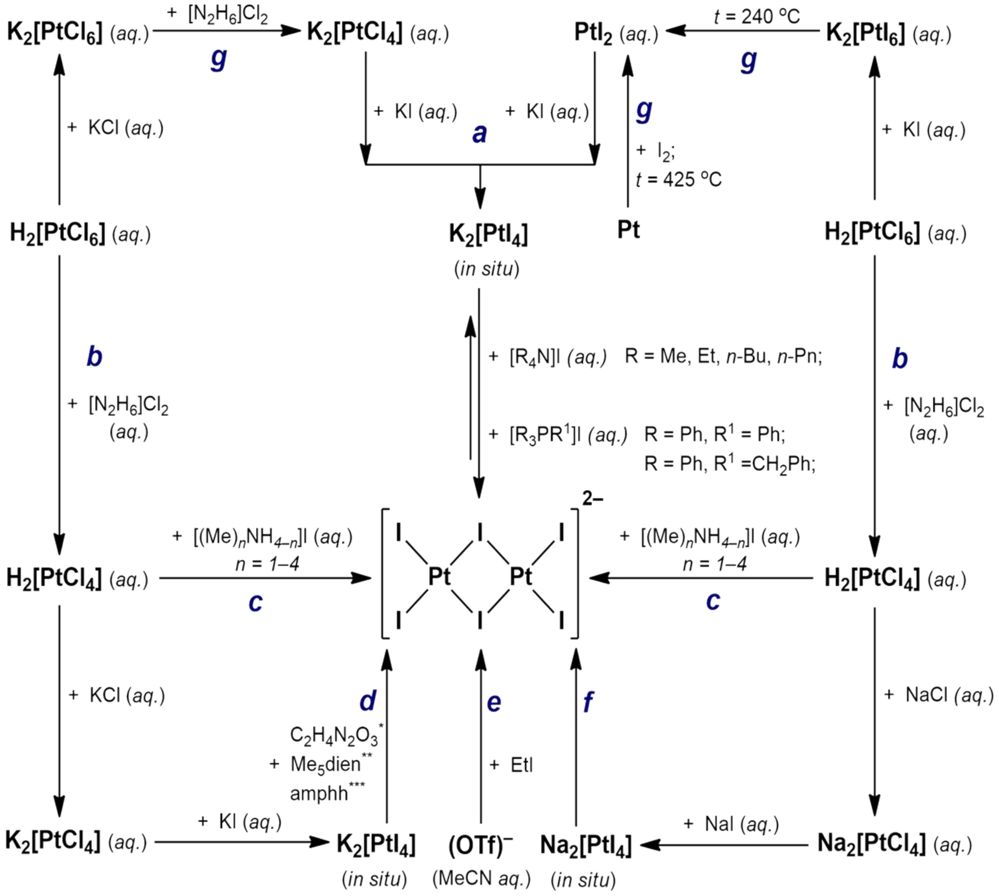

* – barbituric acid; ** – *N,N,N′,N″,N″*-pentamethyldiethylenetriamine; *** – 3-amino-5-methyl-5-phenylhydantoin

Fig. S1. Synthetic routes to complexes featuring the $[Pt_2(\mu\text{-}I)_2I_4]^{2-}$ anion. For synthetic procedures of route *g*, see Ref[9].

Another route to $[Me_nNH_{4-n}]_2[Pt_2(\mu\text{-}I)_2I_4]$ (n = 1–4) includes the addition of aqueous solutions of appropriate $[Me_nNH_{4-n}]I$ to a freshly prepared solution of $H_2[PtCl_4]$ in water (Fig. S1c).[10] The mixed-valence iodoplatinate(II/IV) species such as $[MeNH_3]_4[Pt_3I_{11}]$,[10,11] $[Me_2NH_2]_4[Pt_2I_8]$ (CSD code: WIDMAX),[12] $[Me_3NH]_4[Pt_2I_8]$ (CSD code: WIDMEB),[12] and $[Me_4N]_4[Pt_2I_8]$ (CSD code: WIDMIF),[12] were obtained by the treatment of $H_2[PtCl_6]$ with $[N_2H_6]Cl_2$ followed by addition of the appropriate $[Me_nNH_{4-n}]I$ (Fig. S1bc).

Other reported hexaiododiplatinates(II) such as $K_2[Pt_2(\mu\text{-}I)_2I_4]\bullet 2C_2H_4N_2O_3$ (CSD code: DOZLUZ),[13] $[K(amphh)_2]_2[Pt_2(\mu\text{-}I)_2I_4]$ (CSD code: PIHZAI),[14] and $[PtI(Me_5dien)]_2[Pt_2(\mu\text{-}I)_2I_4]$[15–17] (CSD code: HIXWOA)[17] were precipitated from aqueous solutions of $K_2[PtCl_4]$ containing excess of KI, followed by addition of barbituric acid ($C_2H_4N_2O_3$), 3-amino-5-methyl-5-phenylhydantoin (amphh), or *N,N,N',N'',N''*-pentamethyldiethylenetriamine (Me_5dien), respectively (Fig. S1d). The $Na_2[Pt(\mu\text{-}I)_2I_4]$ complex was prepared *in situ* via substitution of the chlorides from $Na_2[PtCl_4]$ in a saturated solution of NaI in acetone or in water (Fig. S1f).[18] In turn, the complex $[1,4\text{-}\{Pt(MeCN)_2\text{-}(C_6\{CH_2NMe_2\}_4\text{-}2,3,5,6)][Pt_2(\mu\text{-}I)_2I_4]$ (CSD code: HOPRUZ),[19] was obtained by the treatment of $[1,4\text{-}\{Pt(MeCN)_2\text{-}(C_6\{CH_2NMe_2\}_4\text{-}2,3,5,6)](OTf)_2$ with iodoethane in aqueous MeCN (Fig. S1e).

S2. X-ray diffraction and theoretical studies for 1–5

S2.1 Crystal data and structure refinement

Table S1. Crystal data and structure refinement for **1**, **3**–**5**.

	1	**3**	**4**	**5**
CCDC No.	1945398	1945399	1945400	1945401
Empirical formula	$C_8H_{20}I_3NPt$	$C_{16}H_{36}I_3PPt$	$C_{24}H_{20}I_3PPt$	$C_{25}H_{22}I_3PPt$
M_W/g	706.04	835.21	915.16	929.18
T/K	100(2)	100(3)	100(2)	100(2)
Radiation	Mo$K\alpha$ (λ = 0.71073)	Mo$K\alpha$ (λ = 0.71073)	Mo$K\alpha$ (λ = 0.71073)	Cu$K\alpha$ (λ = 1.54184)
Crystal color, shape	brown, prism	clear yellow, prism	green, prism	yellow-green, prism
Crystal size/mm^3	0.328 × 0.125 × 0.088	0.691 × 0.172 × 0.078	0.18 × 0.14 × 0.08	0.22 × 0.16 × 0.10
Crystal system	triclinic	orthorhombic	monoclinic	triclinic
Space group	P-1	Pccn	$P2_1/n$	P-1
a/Å	7.6373(4)	28.7495(4)	12.8781(2)	9.6718(3)
b/Å	8.8684(6)	21.2482(3)	14.4085(2)	10.0466(3)
c/Å	12.8220(9)	15.7822(2)	13.9717(3)	14.9176(3)
α/°	72.104(6)	90	90	78.523(2)
β/°	84.070(6)	90	106.717(2)	82.570(2)
γ/°	67.482(6)	90	90	65.606(3)
V/Å^3	763.31(9)	9641.0(2)	2482.94(8)	1291.92(7)
Z	2	16	4	2
ρ_c/g·cm^{-3}	3.072	2.302	2.448	2.389
μ/mm^{-1}	15.227	9.726	9.455	38.956
F(000)	624.0	6144.0	1664.0	848.0
2Θ range/°	6.172 to 55	3.512 to 63.274	5.096 to 62.778	6.054 to 139.91
Reflections collected	7396	55958	23588	13150
Independent reflections	3495 [R_{int} = 0.0414, R_{sigma} = 0.0657]	14496 [R_{int} = 0.0278, R_{sigma} = 0.0248]	7399 [R_{int} = 0.0275, R_{sigma} = 0.0277]	4887 [R_{int} = 0.0412, R_{sigma} = 0.0397]
Data/restraints/parameters	3495/0/123	14496/0/387	7399/0/262	4887/0/271
Goodness-of-fit on F^2	0.992	1.073	1.072	1.011
Final R indexes [$I \geq 2\sigma(I)$]	R_1 = 0.0393, wR_2 = 0.0735	R_1 = 0.0233, wR_2 = 0.0447	R_1 = 0.0207, wR_2 = 0.0405	R_1 = 0.0262, wR_2 = 0.0669
Final R indexes [all data]	R_1 = 0.0528, wR_2 = 0.0827	R_1 = 0.0328, wR_2 = 0.0472	R_1 = 0.0256, wR_2 = 0.0417	R_1 = 0.0295, wR_2 = 0.0689
Largest diff. peak/hole / e·Å^{-3}	1.98/-2.47	1.22/-1.34	0.57/-0.92	1.06/-1.18

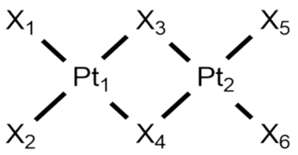

Fig. S2. Atom labeling scheme for $[Pt_2(\mu\text{-}X_2)X_4]^{2-}$ (X = Cl, Br, I) anions.

Table S2. Bond distances and angles for $[Pt_2(\mu\text{-}I)_2I_4]^{2-}$ anions in **1**–**5**.

	Atoms	**1**	**2**[20]	**3**		**4**	**5**
			Distances, Å				
Pt–I$_{bridged}$	Pt1–I3	2.5944(7)	2.5938(3)	2.5897(2)	2.6000(2)	2.6109(2)	2.5999(3)
	Pt1–I4	2.6046(6)[a]	2.5879(3)	2.5935(2)[b]	2.6013(2)[c]	2.60205(19)[d]	2.6041(3)[e]
	Pt2–I3	2.6046(6)[a]	2.5924(3)	2.5936(2)[b]	2.6013(2)[c]	2.60196(19)[d]	2.6040(3)[e]
	Pt2–I4		2.5896(3)				
Pt–I$_{terminal}$	Pt1–I1	2.6032(5)	2.6060(3)	2.5975(2)	2.5934(2)	2.5930(2)	2.6081(3)
	Pt1–I2	2.6003(7)	2.5989(3)	2.5977(2)	2.5989(2)	2.6004(2)	2.5995(3)
	Pt2–I5		2.6069(3)				
	Pt2–I6		2.6004(3)				
			Angles, °				
Interior, °	I3–Pt1–I4	85.20(2)[a]	84.776(8)	84.401(7)[b]	84.451(7)[c]	85.347(6)[d]	84.859(10)[e]
	Pt1–I4–Pt2	94.80(2)[a]	95.328(8)	94.262(7)[b]	95.524(7)[c]	94.652(6)[d]	95.140(10)[e]
	I4–Pt2–I3		84.769(8)				
	Pt2–I3–Pt1		95.115(8)				
Exterior, °	I1–Pt1–I3	90.71(2)	90.905(8)	90.699(7)	91.050(7)	90.869(6)	90.307(10)
	I1–Pt1–I2	92.80(2)	93.904(9)	93.428(7)	93.049(7)	92.241(7)	93.058(11)
	I2–Pt1–I4	91.37(2)[a]	90.449(8)	91.717(7)[b]	91.449(7)[c]	91.541(7)[d]	91.844(10)[e]
	I3–Pt2–I5		91.209(8)				
	I5–Pt2–I6		94.030(9)				
	I4–Pt2–I6		89.997(9)				

[a] 1-X,1-Y,1-Z; [b] 1/2-X,1/2-Y,+Z; [c] 1/2-X,3/2-Y,+Z; [d] 2-X,1-Y,1-Z; [e] -X,2-Y,-Z.

S2.2 Comparison of bridged and terminal Pt–X (X = Cl, Br, I) bond lengths

In **1**–**5**, the anions are planar, and maximum deviation from the planarity (0.394 Å) is observed for the terminal iodides of **3**. The crystal structure of **3** consists of two crystallographic independent $[Pt_2(\mu\text{-}I)_2I_4]^{2-}$ units, in one of which all terminal Pt–I bond lengths are slightly longer, within 3σ, than the Pt–$I_{bridged}$ distances, while in another anion a shortening of the Pt–$I_{terminal}$ bonds is observed. In the crystal structure of **2**, all Pt–$I_{terminal}$ distances are also longer, taking into account the 3σ criterion, than the Pt–$I_{bridged}$ bond lengths. The same tendency in general remains in the XRD structures of **1** and **5**. Nevertheless, in **4**, all Pt–$I_{bridged}$ distances are slightly longer, than Pt–$I_{terminal}$ bonds. In previously reported five structures $(Cation)_2[Pt_2(\mu\text{-}I_2)I_4]$,[4,13,14,17,19] Pt–$I_{bridged}$ and Pt–$I_{terminal}$ distances are equal within 3σ, except DOZLUZ,[13] where two Pt–$I_{bridged}$ distances, viz. Pt1–I3 and Pt1–I4, are somehow longer than Pt2–I5 and Pt2–I6 terminal bond lengths, while in HIXWOA[17] and PIHZAI[14] a shortening of the Pt–$I_{bridged}$ bonds is observed (Table S3). Thus, taking into account these data, in the vast majority of cases there is a stretching of the terminal bonds in the $[Pt_2(\mu\text{-}I)_2I_4]^{2-}$ anions.

Inspection of the available data on the crystal structures of similar bromide[21–24] and chloride[25,26] complexes revealed the following results (Table S3). In the XRD structures of ETABPT01[21] and GAPGUC,[22] Pt–$Br_{bridged}$ and Pt–$Br_{terminal}$ are equal within 3σ, except Pt1–Br3 and Pt2–Br4 bridged bonds, which are longer than terminal bond lengths. In another two literature structures, viz. CUHXAF[23] and HEKYAZ,[24] a stretching of all Pt–$Br_{bridged}$ bonds is observed. In the crystal structures of two hexachlorodiplatinates(II) (DMCPRP10[25] and KOWCII[26]), all Pt–$Cl_{bridged}$ bonds are longer, taking into account the 3σ criterion, than the Pt–$Cl_{terminal}$ distances.

Thus, in accord with these data, the terminal bond lengths increase along with the increase of covalent halide radii (Cl > Br > I).

Table S3. Bond distances (Å) and angles (°) for $[\mathrm{Pt_2}(\mu\text{-}\mathrm{X_2})\mathrm{X_4}]^{2-}$ (X = Cl, Br, I) anions.

	Atoms	$[\mathrm{Pt_2}(\mu\text{-}\mathrm{I_2})\mathrm{I_4}]^{2-}$					$[\mathrm{Pt_2}(\mu\text{-}\mathrm{Br_2})\mathrm{Br_4}]^{2-}$				$[\mathrm{Pt_2}(\mu\text{-}\mathrm{Cl_2})\mathrm{Cl_4}]^{2-}$	
		CODHIM	DOZLUZ	HIXWOA	HOPRUZ	PIHZAI	CUHXAF	ETABPT01	GAPGUC	HEKYAZ	DMCPRP10	KOWCII
Distances, Å												
Pt–X$_{\text{bridged}}$	Pt1–X3	2.553(4)	2.601(2)^a	2.586(1)	2.5995(14)	2.5898(13)	2.4403(6)	2.446(5)	2.410(7)	2.4578(9)	2.3368(13)	2.3267(15)
	Pt1–X4	2.562(4)	2.601(2)	2.595(1)^b	2.6001(17)^c	2.5938(8)^d	2.4427(6)^e	2.439(5)^f	2.402(9)^g	2.4641(9)^h	2.3268(18)	2.3302(14)^i
	Pt2–X3	2.560(4)	2.596(2)^a	2.595(1)^b	2.6001(17)^c	2.5938(8)^d	2.4427(6)^e	2.439(5)^f	2.402(9)^g	2.4641(9)^h	2.3195(17)	2.3302(14)^i
	Pt2–X4	2.562(4)	2.596(2)								2.3322(12)	
Pt–X$_{\text{terminal}}$	Pt1–X1	2.569(4)	2.594(3)^a	2.596(1)	2.601(2)	2.5970(8)	2.4087(6)	2.411(5)	2.352(9)	2.4168(9)	2.2682(18)	2.2762(14)
	Pt1–X2	2.575(4)	2.594(3)	2.601(1)^b	2.6011(15)^c	2.5918(14)^d	2.4183(6)^e	2.415(5)^f	2.377(7)^g	2.4198(8)^h	2.2789(13)	2.2783(15)^i
	Pt2–X5	2.562(4)	2.581(3)	2.601(1)^b	2.6011(15)^c	2.5918(14)^d	2.4183(6)^e	2.415(5)^f	2.377(7)^g	2.4198(8)^h	2.2787(13)	2.2783(15)^i
	Pt2–X6	2.577(4)	2.581(3)								2.2647(13)	
Angles, °												
Interior, °	X3–Pt1–X4	84.5(1)	85.2(1)	84.61(3)^b	84.21(5)^c	84.79(3)^d	85.352(19)^e	85.4(3)^f	85.6(3)^g	85.29(3)^h	84.9(1)	84.47(6)^i
	Pt1–X4–Pt2	95.4(1)	94.8(1)^a	95.39(3)^b	95.79(5)^c	95.21(3)^d	94.648(19)^e	94.6(3)^f	94.4(3)^g	94.72(3)^h	94.4(1)	95.53(6)^i
	X4–Pt2–X3	84.4(1)	85.3(1)								85.2(1)	
	Pt2–X3–Pt1	95.7(1)	94.8(1)^a								94.5(1)	
Exterior, °	X1–Pt1–X3	90.2(1)	90.9(1)^a	90.29(3)^b	92.46(5)	92.31(3)	90.36(2)	91.2(3)	91.6(3)	91.73(3)	91.4(1)	92.77(5)
	X1–Pt1–X2	94.0(1)	93.1(1)^a	94.13(3)	91.80(5)	92.01(3)	92.74(2)	92.4(3)	90.6(3)	91.81(3)	92.6(1)	90.14(5)
	X2–Pt1–X4	91.4(1)	90.9(1)	90.96(3)	91.52(5)^c	90.85(3)^d	91.59(2)^e	91.1(3)^f	92.2(3)^g	91.16(3)^h	91.0(1)	92.62(5)^i
	X3–Pt2–X5	90.7(1)	90.7(1)^a		91.52(5)^c	90.85(3)^d	91.59(2)^e	91.1(3)^f	92.2(3)^g	91.16(3)^h	91.1(1)	92.62(5)^i
	X5–Pt2–X6	93.9(1)	93.1(1)								92.2(1)	
	X4–Pt2–X6	91.1(1)	90.7(1)								91.4(1)	
Refs		4	13	17	19	14	23	21	22	24	25	26

^{a} -X,+Y,1/2-Z; ^{b} 1-X,-Y,1-Z; ^{c} -X,-Y,-Z; ^{d} 1-X,2-Y,1-Z; ^{f} -X,-Y,-Z; ^{g} 2-X,-Y,-Z; ^{h} 1-X,1-Y,-Z; ^{i} 1-X,-Y,-Z.

S2.3 Hydrogen bonds in 1–5

Table S4. Parameters of C–H•••X–Y (X = I, Pt; Y = I, Pt) HBs in **1**–**3**, **5**.

Structure	Contact	*d*(H•••X), Å	*d*(C•••X), Å	∠(C–H•••X),°	R[a]
1	C1–H1A•••I3–Pt1	3.1234(5)	3.949(7)	143.9(5)	0.95
	C5–H5B•••I3–Pt1	3.1483(7)	4.036(11)	153.1(5)	0.98
2	C25–H25A•••I6–Pt2	3.0389(3)	3.969(4)	161.0(2)	0.96
	C21–H21B•••I2–Pt1	3.0795(4)	3.985(3)	155.94(16)	0.97
	C25–H25B•••I1–Pt1	3.1134(4)	4.039(4)	160.2(2)	0.98
	C3–H3A•••I2–Pt1	3.1462(4)	3.969(4)	143.6(2)	0.99
	C17–H17B•••I5–Pt2	3.1714(3)	4.099(3)	160.60(18)	0.97
	C18–H18B•••I1–Pt1	3.1785(3)	3.897(4)	132.3(3)	0.97
3	C13–H13A•••I1–Pt1	3.0529(5)	3.930(3)	148.37(16)	0.99
	C25–H25B•••I6–Pt2	3.1593(3)	4.028(3)	147.29(17)	1.00
5	C14–H14•••I2–Pt1	3.0185(4)	3.757(6)	137.4(3)	0.95
	C12–H12•••I1–Pt1	3.0724(3)	3.928(4)	153.8(4)	1.00
	C19–H19•••Pt1	3.738(4)	2.8566(2)	151.5(3)	0.99
				110<∠<180[b]	

[a] R is interatomic distance to vdW sum ratio,[27] $\Sigma_{vdW}R$, are: $R_{vdW}(H) + R_{vdW}(I) = 3.18$ Å, $R_{vdW}(H) + R_{vdW}(Pt) = 2.95$ Å.

[b] Comparison with the typical HB angles.

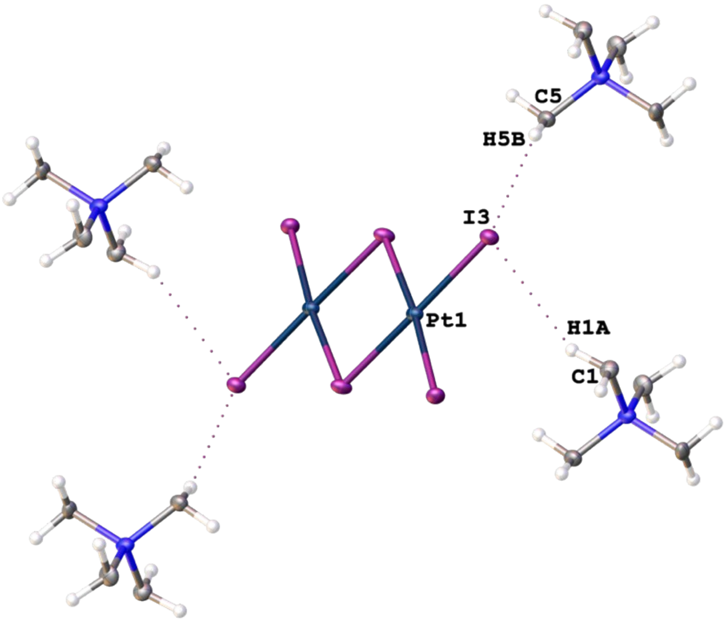

Fig. S3. HBs in **1** between the Hs of [Et$_4$N]$^+$ (peripheral ethyl groups of the [Et$_4$N]$^+$ were omitted for clarity) and the terminal iodide ligands of [Pt$_2$(μ-I$_2$)I$_4$]$^{2-}$. The contacts shorter Bondi vdW radii sums,[27] $\Sigma_{vdW}R$, are given by dotted lines. Thermal ellipsoids are shown with the 50% probability.

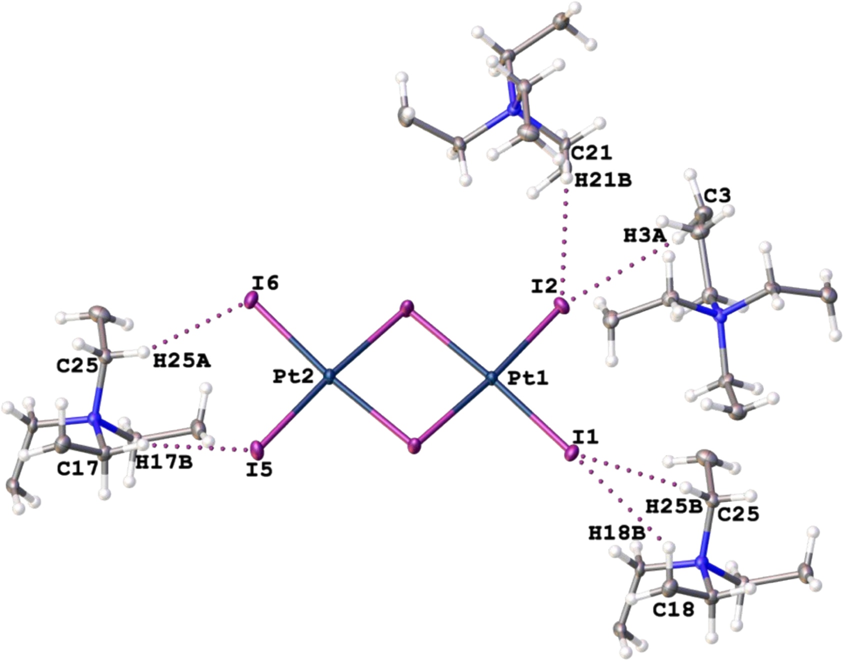

Fig. S4. HBs in **2** between the Hs of [nBu$_4$N]$^+$ (peripheral ethyl groups of the [nBu$_4$N]$^+$ were omitted for clarity) and the terminal iodide ligands of [Pt$_2$(μ-I$_2$)I$_4$]$^{2-}$. The contacts shorter Σ_{vdW}R are given by dotted lines. Thermal ellipsoids are shown with the 50% probability.

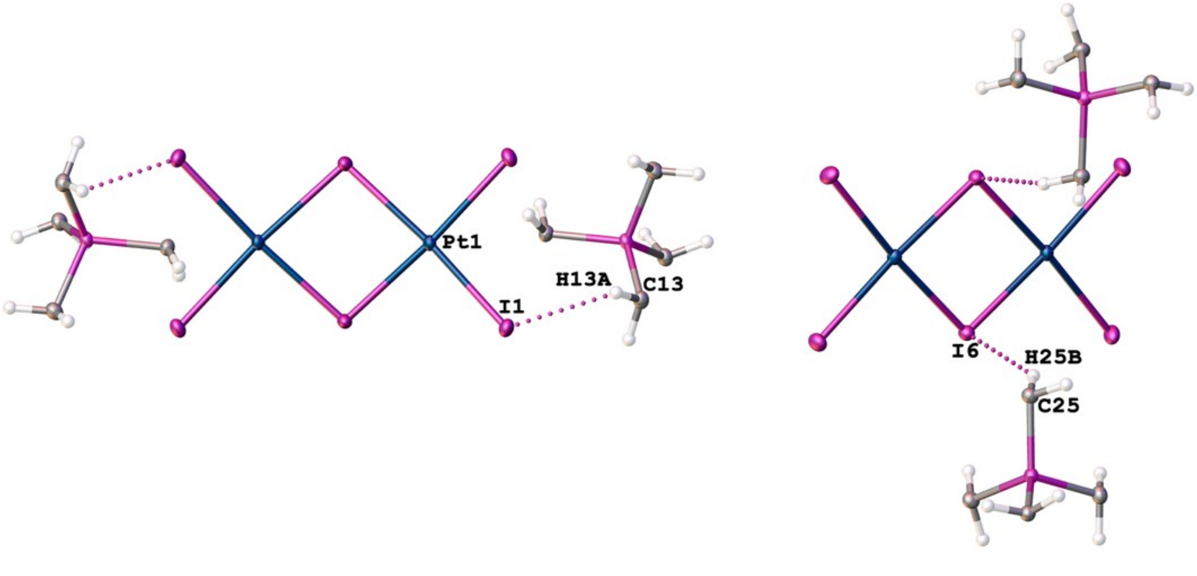

Fig. S5. HBs in **3** between the H atoms of [n-Bu$_4$P]$^+$ (peripheral propyl groups of the [n-Bu$_4$P]$^+$ were omitted for clarity) and the I ligands of [Pt$_2$(μ-I)$_2$I$_4$]$^{2-}$. The contacts shorter Σ_{vdW}R are given by dotted lines. Thermal ellipsoids are shown with the 50% probability.

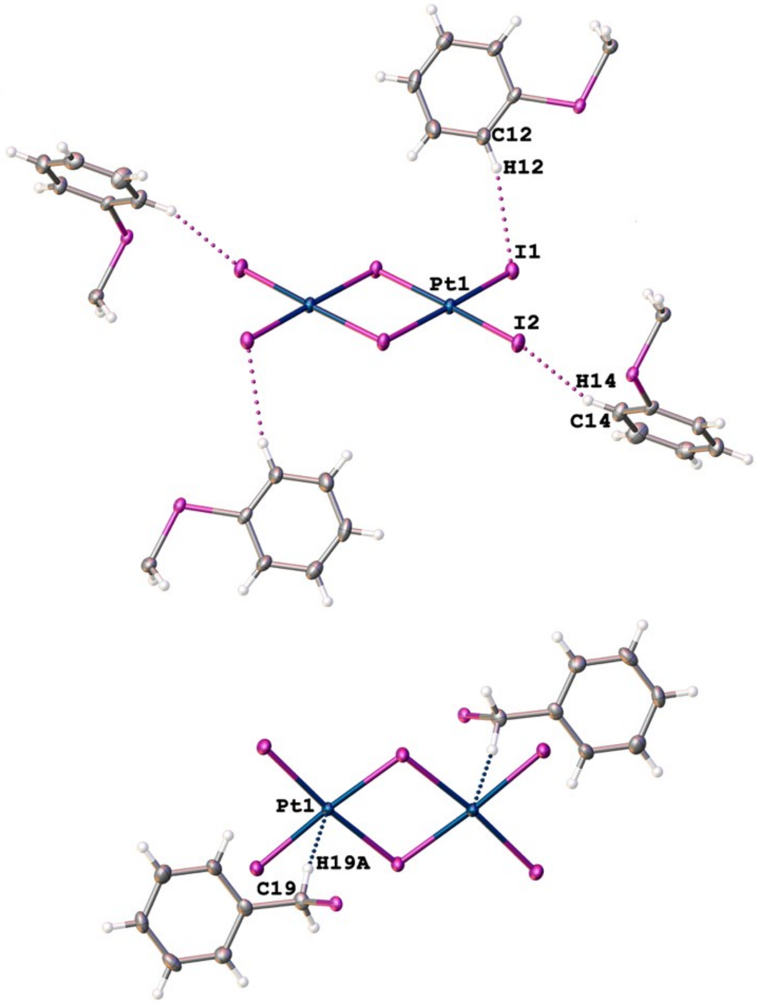

Fig. S6. HBs between the Hs of $[Ph_3CH_2P]^+$ (3 phenyl groups were omitted for clarity) and terminal I ligands of $[Pt_2(\mu\text{-}I_2)I_4]^{2-}$ (top) and between the Hs of the cations (3 phenyl groups were omitted for clarity) and the Pt centers of $[Pt_2(\mu\text{-}I_2)I_4]^{2-}$ (bottom) in **5**. The contacts shorter $\Sigma_{vdW}R$ are given by dotted lines. Thermal ellipsoids are shown with the 50% probability.

S2.4 Theoretical calculations for the $[Pt_2(\mu\text{-}X_2)X_4]^{2-}$ (X = Cl, Br, I) model species

Table S5. Cartesian atomic coordinates for all calculated optimized equilibrium model structures.

Atom	X	Y	Z
$[Pt_2(\mu\text{-}Br_2)Br_4]^{2-}$			
Pt	-0.827046	1.491465	-0.863887
Br	0.041738	0.892199	1.499589
Br	-1.629932	1.924111	-3.208274
Br	-1.540324	3.778727	-0.098414
Pt	0.827046	-1.491465	0.863887
Br	-0.041738	-0.892199	-1.499589
Br	1.629932	-1.924111	3.208274
Br	1.540324	-3.778727	0.098414
$[Pt_2(\mu\text{-}Cl_2)Cl_4]^{2-}$			
Pt	-0.797381	1.442124	-0.837877
Cl	0.033329	0.848182	1.429957
Cl	-1.555588	1.856101	-3.066329
Cl	-1.484855	3.615818	-0.115915
Pt	0.797381	-1.442124	0.837877
Cl	-0.033329	-0.848182	-1.429957
Cl	1.555588	-1.856101	3.066329
Cl	1.484855	-3.615818	0.115915
$[Pt_2(\mu\text{-}I_2)I_4]^{2-}$			
Pt	-2.011074	0.000056	-0.000213
I	0.000024	1.829886	-0.000918
I	-3.870011	-1.936526	0.000621
I	-3.870230	1.936419	0.000615
Pt	2.011063	-0.000010	-0.000123
I	-0.000024	-1.829858	-0.000989
I	3.870149	1.936450	0.000553
I	3.870109	-1.936439	0.000614

S3. X-ray diffraction and computational studies for the obtained adducts

S3.1 Crystal data and structure refinement

Table S6. Crystal data and structure refinement for the obtained adducts.

	1•2(1,3,5-FIB)	**1**•2IPFB	**2**•2(1,4-FIB)	**3**•C_2I_4
CCDC No.	1945444	1945452	1945453	1945454
Empirical formula	0.331 × 0.190 × 0.088	$C_{14}H_{20}F_5I_4NPt$	$C_{22}H_{36}F_4I_5NPt$	$C_{34}H_{72}I_{10}P_2Pt_2$
M_W/g	2431.60	1000.00	1220.11	2202.03
T/K	100(2)	100(2)	100(2)	100(2)
Radiation	Mo$K\alpha$ (λ = 0.71073)	Mo$K\alpha$ (λ = 0.71073)	Mo$K\alpha$ (λ = 0.71073)	Mo$K\alpha$ (λ = 0.71073)
Crystal color, shape	clear dark brown, block	brown, prism	brown, prism	brown, prism
Crystal size/mm^3	0.331 × 0.190 × 0.088	0.15 × 0.11 × 0.08	0.36 × 0.28 × 0.19	0.367 × 0.091 × 0.052
Crystal system	triclinic	triclinic	triclinic	triclinic
Space group	P-1	P-1	P-1	P-1
a/Å	9.0752(3)	7.4631(3)	9.4019(3)	10.6311(3)
b/Å	14.0688(3)	8.8084(3)	9.4572(5)	11.7665(3)
c/Å	20.5122(4)	19.7624(7)	18.4950(7)	22.2710(5)
α/°	103.355(2)	84.162(3)	81.698(4)	84.641(2)
β/°	95.542(2)	80.035(3)	85.055(3)	87.252(2)
γ/°	97.711(2)	67.019(3)	77.612(3)	89.297(2)
V/Å^3	2502.88(11)	1177.15(8)	1586.78(12)	2770.45(12)
Z	2	2	2	2
ρ_c/g·cm^{-3}	3.227	2.821	2.554	2.640
μ/mm^{-1}	13.029	11.243	9.321	10.695
F(000)	2136.0	892.0	1108.0	1984.0
2Θ range/°	5.402 to 55	5.372 to 53.986	5.084 to 56.998	5.158 to 55
Reflections collected	23042	17540	14669	47428
Independent reflections	11490 [R_{int} = 0.0345, R_{sigma} = 0.0461]	5152 [R_{int} = 0.0337, R_{sigma} = 0.0267]	8034 [R_{int} = 0.0251, R_{sigma} = 0.0418]	12715 [R_{int} = 0.0268, R_{sigma} = 0.0262]
Data/restraints/parameters	11490/0/460	5152/0/225	8034/0/302	12715/0/441
Goodness-of-fit on F^2	1.059	1.091	1.036	1.071
Final R indexes [$I \geq 2\sigma(I)$]	R_1 = 0.0294, wR_2 = 0.0591	R_1 = 0.0276, wR_2 = 0.0703	R_1 = 0.0254, wR_2 = 0.0470	R_1 = 0.0235, wR_2 = 0.0460
Final R indexes [all data]	R_1 = 0.0335, wR_2 = 0.0614	R_1 = 0.0291, wR_2 = 0.0713	R_1 = 0.0310, wR_2 = 0.0492	R_1 = 0.0296, wR_2 = 0.0479
Largest diff. peak/hole / e·Å^{-3}	1.83/-1.83	2.34/-1.57	1.32/-0.94	2.02/-1.95

Table S7. Bond distances and angles for $[\mathrm{Pt}_2(\mu\text{-I})_2\mathrm{I}_4]^{2-}$ anions in the adducts.

	Atoms	**1**•2(1,3,5-FIB)	**1**•2IPFB	**2**•2(1,4-FIB)	**3**•C_2I_4
Distances, Å					
Pt–$I_{bridged}$	Pt1–I3	2.6039(4)	2.5964(3)	2.5931(3)	2.5998(3)
	Pt1–I4	2.5952(4)	2.5964(4)[a]	2.5952(3)[b]	2.5999(3)
	Pt2–I3	2.5925(4)	2.5964(4)[a]	2.5953(3)[b]	2.5933(3)
	Pt2–I4	2.5982(4)			2.5988(3)
Pt–$I_{terminal}$	Pt1–I1	2.6027(4)	2.5964(3)	2.5992(3)	2.5918(3)
	Pt1–I2	2.6119(4)	2.6004(3)	2.6004(3)	2.5969(3)
	Pt2–I5	2.6038(4)			2.6034(3)
	Pt2–I6	2.5995(4)			2.5952(3)
Angles, °					
Interior, °	I3–Pt1–I4	84.911(13)	85.177(11)[a]	84.600(10)[b]	84.770(10)
	Pt1–I4–Pt2	94.631(13)	94.823(11)[a]	95.401(10)[b]	95.058(10)
	I4–Pt2–I3	85.082(13)			84.924(10)
	Pt2–I3–Pt1	94.559(13)			95.194(10)
Exterior, °	I1–Pt1–I3	90.248(13)	89.821(11)	91.429(10)	91.131(10)
	I1–Pt1–I2	93.548(13)	93.235(11)	93.113(10)	91.926(10)
	I2–Pt1–I4	91.314(13)	91.845(11)[a]	91.460(10)[b]	92.169(10)
	I3–Pt2–I5	92.468(13)			91.523(10)
	I5–Pt2–I6	91.894(13)			92.501(10)
	I4–Pt2–I6	90.566(13)			91.051(10)

[a] -1-X,1-Y,2-Z; [b] -X,1-Y,-Z.

S3.2 Hirshfeld surface analysis

Table S8. Results of the Hirshfeld surface analysis for anionic parts in the XRD structures of the adducts.

XRD structure	Contributions of different intermolecular contacts to the molecular Hirshfeld surface[*]
1•2(1,3,5-FIB)	I–H 62.3%, I–I 19.5%, Pt–H 9.9%, I–F 4.8%, I–C 3.4%
1•2IPFB	I–H 69.4%, I–I 13.8%, Pt–H 10.0%, I–F 6.8%
2•2(1,4-FIB)	I–H 76.2%, I–I 12.4%, Pt–H 9.6%, I–F 1.3%
3•C_2I_4	I–H 82.5%, I–I 7.6%, Pt–H 9.9%

[*] The contributions of all other intermolecular contacts do not exceed 1%.

S3.3 Hydrogen bonds in the adducts

In the molecular structures of **1**•2(1,3,5-FIB) and **1**•2IPFB, the $[Et_4N]^+$ are associated with the $[Pt_2(\mu\text{-}I)_2I_4]^{2-}$ via C–H•••I–Pt HBs formed between the terminal iodide ligands and the Hs of the cations (Fig. S7–S8, Table S9). Additionally, the cations are linked with $R^{EWG}I$ XB donors, viz. 1,3,5-FIB and IPFB, through C–H•••F–C HBs (Fig. S7–S8, Table S9).

The molecular structure of **2**•2(1,4-FIB) exhibits interionic and intermolecular C–H•••I–X (X = Pt, C) HBs, formed, on the one hand, between the Hs of the cations and the iodide ligands of the anions (Fig. S9a; Table S9) and, on the other hand, between the H atom of $[n\text{-}Bu_4N]^+$ and the I center of 1,4-FIB; the cations are also linked to 1,4-FIB via C–H•••F–C HBs (Fig. S9b; Table S9).

In **3**•C_2I_4, the $[n\text{-}Bu_4P]^+$ is associated with the $[Pt_2(\mu\text{-}I)_2I_4]^{2-}$ through C24–H24C•••I6–Pt2 HB formed between the H of the cation and the terminal iodide ligand of the anion (Fig. S10b; Table S9), as well as via C13–H13A•••Pt1 HB between the Pt center and the H atom of the $[n\text{-}Bu_4P]^+$ (Fig. S10a; Table S9).

Table S9. Parameters of C–H•••X–Y (X = I, F, Pt; Y = Pt, C, I) HBs in the adducts.

Structure	**Contact**	***d*(H•••X), Å**	***d*(C•••X), Å**	**∠(C–H•••X),°**	**R**[a]
1•2(1,3,5-FIB)	C3–H3A•••I2–Pt1	3.0254(4)	3.944(5)	154.8(4)	0.95
	C5–H5A•••I1–Pt1	3.1235(4)	3.977(6)	145.2(3)	0.98
	C13–H13B•••I5–Pt2	3.1786(4)	3.872(6)	128.4(3)	1.00
	C4–H4A•••F5S–C10S	2.451(4)	3.220(7)	134.9(3)	0.92
	C5–H5B•••F1S–C2S	2.470(3)	3.169(7)	127.2(3)	0.93
	C4–H4C•••F1S–C2S	2.502(3)	3.449(6)	162.3(4)	0.94
	C16–H16A•••F4S–C8S	2.524(3)	3.501(7)	176.2(4)	0.95
	C13–H13B•••F4S–C8S	2.530(3)	3.320(7)	136.6(3)	0.95
	C16–H16B•••F3S–C6S	2.530(3)	3.056(7)	113.4(3)	0.95
	C11–H11A•••F2S–C4S	2.559(3)	3.255(6)	127.3(4)	0.96
1•2IPFB	C1–H1B•••I2–Pt1	3.0639(3)	3.897(5)	144.8(4)	0.96
	C5–H5B•••I2–Pt1	3.0816(4)	4.001(6)	158.7(4)	0.97
	C7–H7B•••I3–Pt1	3.0929(4)	3.837(7)	134.8(3)	0.97
	C3–H3A•••I3–Pt1	3.1371(3)	4.024(5)	152.9(3)	0.99
	C3–H3B•••F3S–C4S	2.592(5)	3.421(8)	143.4(4)	0.97
2•2(1,4-FIB)	C1–H1B•••I1S–C1S	3.1545(3)	4.028(4)	150.5(2)	0.99
	C5–H5A•••I3–Pt1	3.1698(3)	3.816(4)	125.6(3)	1.00
	C2–H2A•••F3S–C5S	2.556(2)	3.518(4)	171.0(3)	0.96
	C4–H4B•••F2S–C3S	2.594(2)	3.466(5)	151.1(3)	0.97
3•C_2I_4	C24–H24C•••I6–Pt2	3.1674(4)	3.998(4)	143.4(3)	1.00
	C13–H13A•••Pt1	2.9261(3)	3.912(4)	173.9(2)	0.99
				110<∠<180[b]	

[a] R is interatomic distance to vdW sum ratio, the sums of Bondi vdW radii[27] are: $R_{vdW}(H) + R_{vdW}(I) = 3.18$ Å, $R_{vdW}(H) + R_{vdW}(F) = 2.67$ Å, $R_{vdW}(H) + R_{vdW}(Pt) = 2.95$ Å.

[b] Comparison with the typical HB angles.

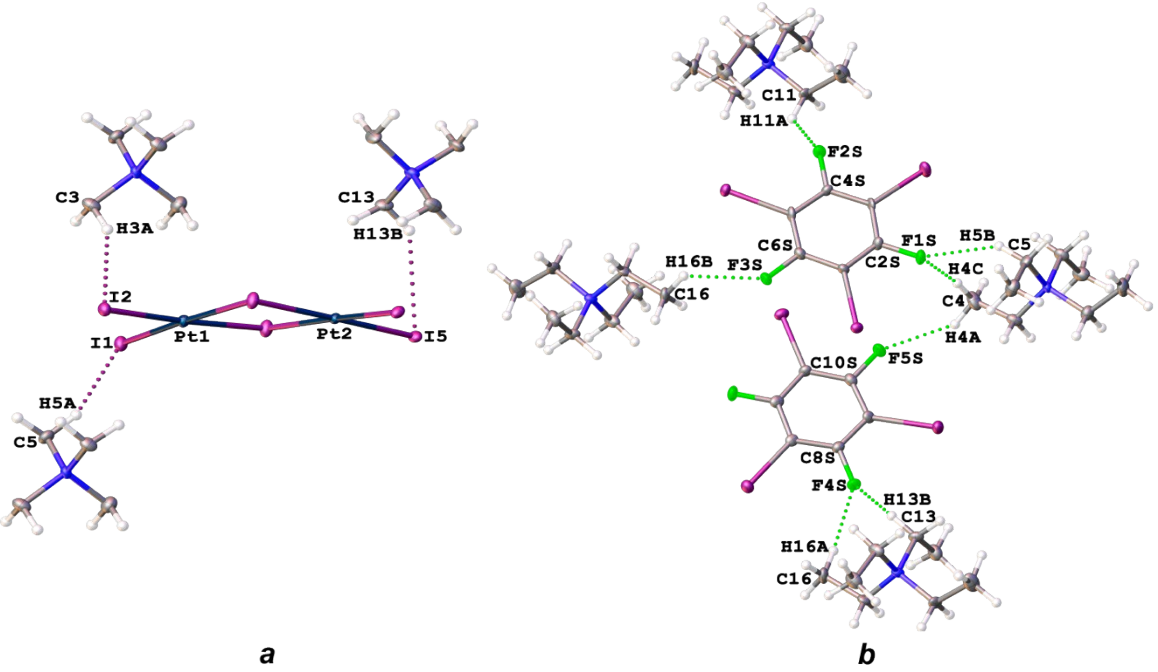

Fig. S7. HBs in **1**•2(1,3,5-FIB): (*a*) between the Hs of $[Et_4N]^+$ (peripheral ethyl groups of the $[Et_4N]^+$ were omitted for clarity) and the terminal iodide ligands of $[Pt_2(\mu\text{-}I_2)I_4]^{2-}$; (*b*) between the Hs of the cations and the F atoms of 1,3,5-FIBs. The contacts shorter $\Sigma_{vdW}R$ are given by dotted lines. Thermal ellipsoids are shown with the 50% probability.

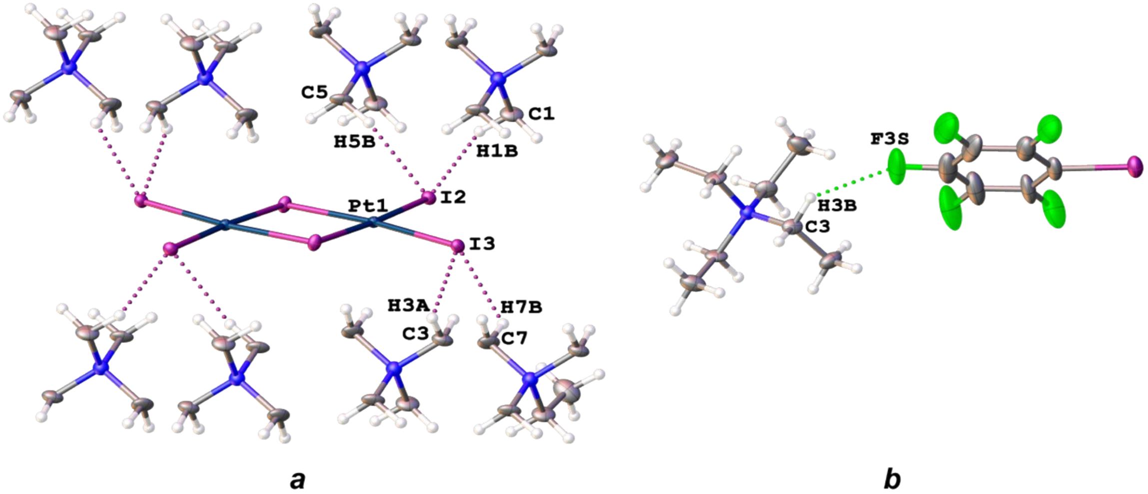

Fig. S8. HBs in **1**•2IPFB: (*a*) between the Hs of $[Et_4N]^+$ (peripheral ethyl groups of the $[Et_4N]^+$ were omitted for clarity) and the terminal iodide ligands of $[Pt_2(\mu\text{-}I_2)I_4]^{2-}$; (*b*) between the H atom of the cation and the F of IPFB. The contacts shorter $\Sigma_{vdW}R$ are given by dotted lines. Thermal ellipsoids are shown with the 50% probability.

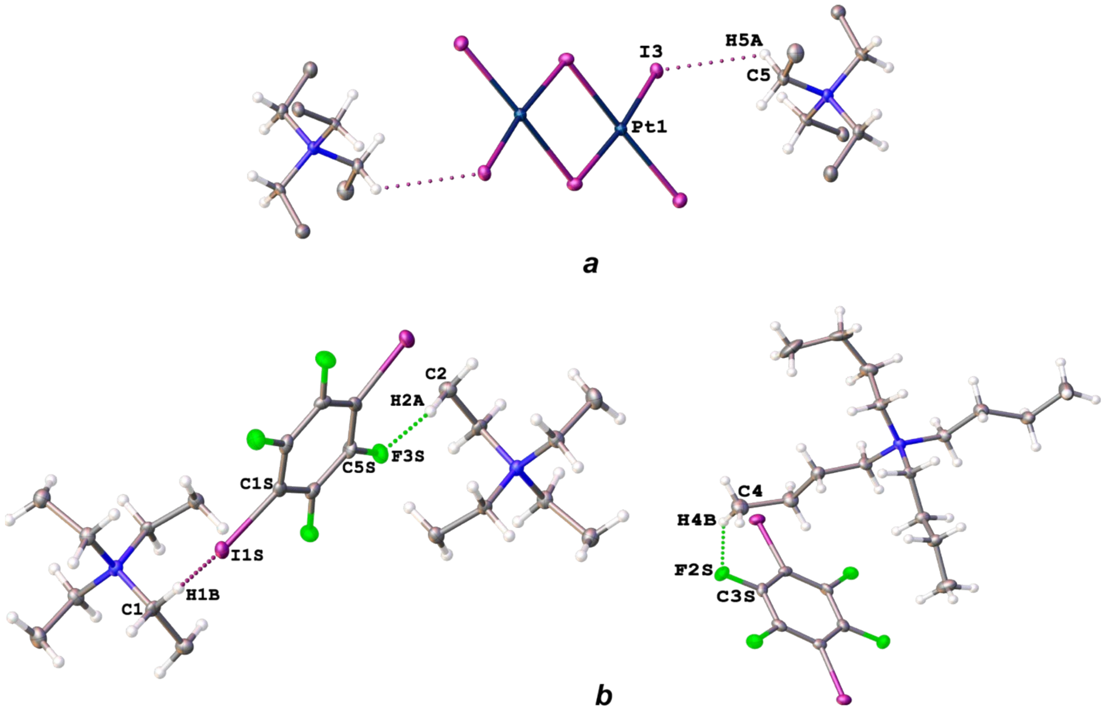

Fig. S9. HBs in **2**•2(1,4-FIB): (*a*) between the H atoms of $[n\text{-Bu}_4\text{N}]^+$ (peripheral ethyl groups and 2-H atoms of the $[n\text{-Bu}_4\text{N}]^+$ were omitted for clarity) and the I ligands of $[\text{Pt}_2(\mu\text{-I})_2\text{I}_4]^{2-}$; (*b*) between the Hs of the cations (on left side peripheral ethyl groups of the $[n\text{-Bu}_4\text{N}]^+$ were omitted for clarity) and the halogens atoms of 1,4-FIB. The contacts shorter Σ_{vdW}R are given by dotted lines. Thermal ellipsoids are shown with the 50% probability.

Fig. S10. HBs (*a*) between the H atom of $[n\text{-Bu}_4\text{P}]^+$ (3 peripheral ethyl groups were omitted for clarity) and the I ligand of $[\text{Pt}_2(\mu\text{-I}_2)\text{I}_4]^{2-}$, and (*b*) between the H of the cation (peripheral ethyl groups were omitted for clarity) and the Pt center of $[\text{Pt}_2(\mu\text{-I}_2)\text{I}_4]^{2-}$ in **3**•C_2I_4. The contacts shorter Σ_{vdW}R are given by dotted lines. Thermal ellipsoids are shown with the 50% probability.

S3.4 π-Interactions in 1•2(1,3,5-FIB) and 2•2(1,4-FIB)

Another type of noncovalent interactions includes C•••I–C short contact formed between the I atom and the electron deficient π-system of 1,3,5-FIBs in **1**•2(1,3,5-FIB) (Fig. S11a). The C6S•••I6S–C11S distance (3.662(5) Å) is less than the sum of Bondi vdW radii[27] ($R_{vdW}(I) + R_{vdW}(C) = 3.68$ Å) and the angle ∠(C6S•••I6S–C11S) is equal to 90.53(17)°. The observed C6S•••I6S–C11S weak contact belong to the category of lp(I)–π interactions involving 1,3,5-FIB.

In **2**•2(1,4-FIB), 1,4-FIB molecules are linked to each other via C3S•••C3S short contact (*d* = 3.397(8) Å; Fig. S11b) between the π-systems of the fluorinated iodoarenes. All characteristic parameters of this interaction, namely plane centroid to plane centroid distance (4.485(4) Å), distance between centroid of one ring to plane of another (3.296(7) Å), plane to plane shift (3.041(7) Å), angle between ring planes (0.0(2)°), and twist angle (0.0(9)°), indicate that it belongs to π–π contact according to the criteria for π-stacking.[28–30] The existence of C6S•••I6S–C11S and C3S•••C3S weak contacts was additionally confirmed by our theoretical calculations (Section 2.6).

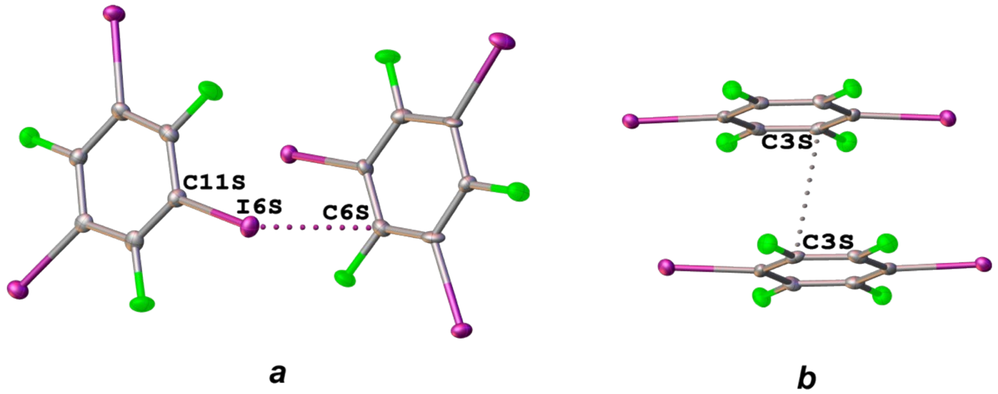

Fig. S11. π-Interactions in (*a*) **1**•2(1,3,5-FIB) and (*b*) **2**•2(1,4-FIB).

S3.5 Theoretical study of noncovalent interactions in crystal structures of the adducts

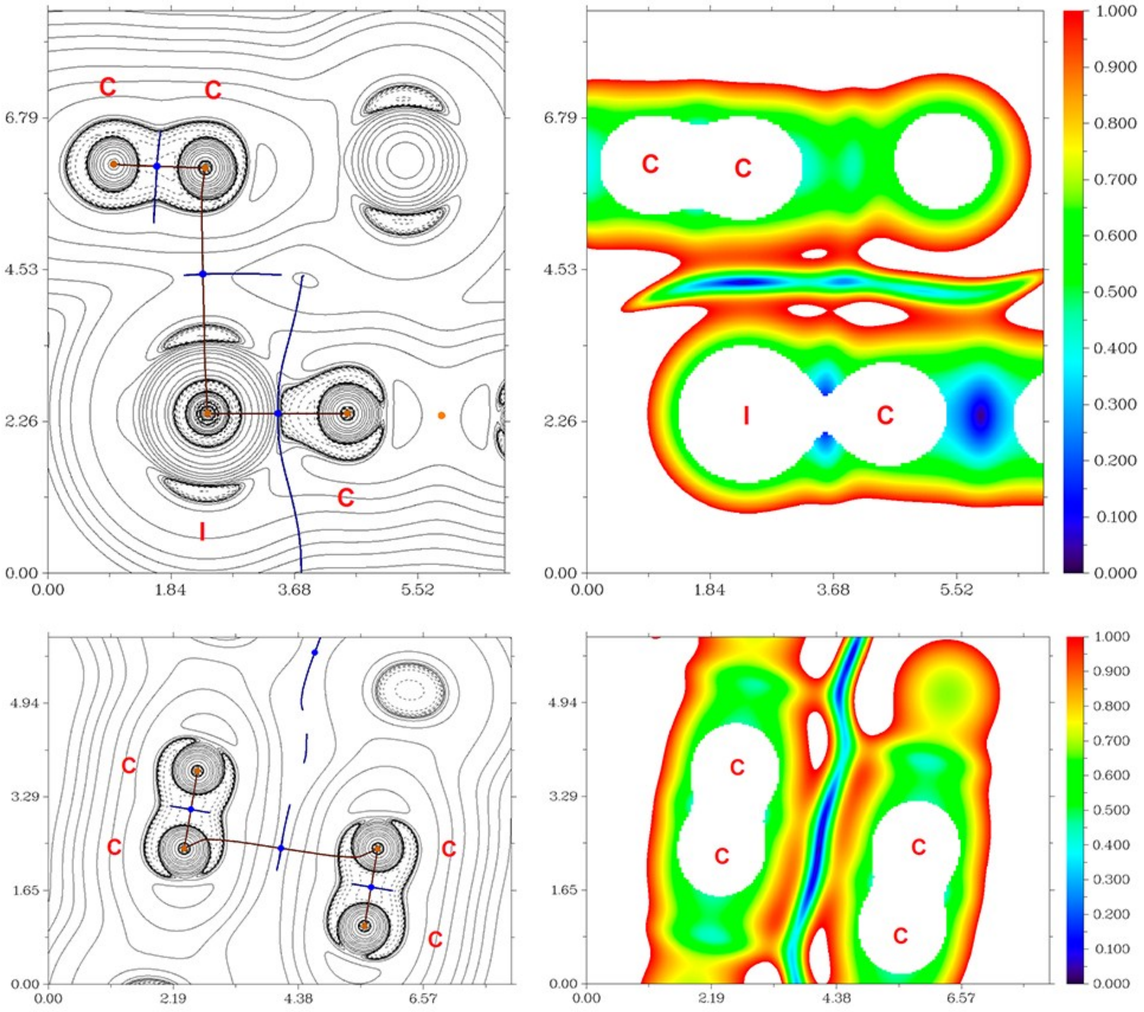

Fig. S12. Contour line diagram of the Laplacian distribution $\nabla^2\rho(\mathbf{r})$, bond paths and selected zero-flux surfaces (left) and RDG isosurface (right) referring to C6S•••I6S–C11S lp(I)–π short contact in $[Pt_2(\mu\text{-}I)_2I_4]^{2-}$•(1,3,5-FIB)$_5$ (top) and C3S•••C3S π-interactions in $[n\mathrm{Bu}_4\mathrm{N}]^+_2[Pt_2(\mu\text{-}I)_2I_4]^{2-}$•(1,4-FIB)$_4$ (bottom). Bond critical points (3, –1) are shown in blue, nuclear critical points (3, –3) – in pale brown, ring critical points (3, +1) – in orange. Length units – Å, RDG isosurface values are given in a.u.

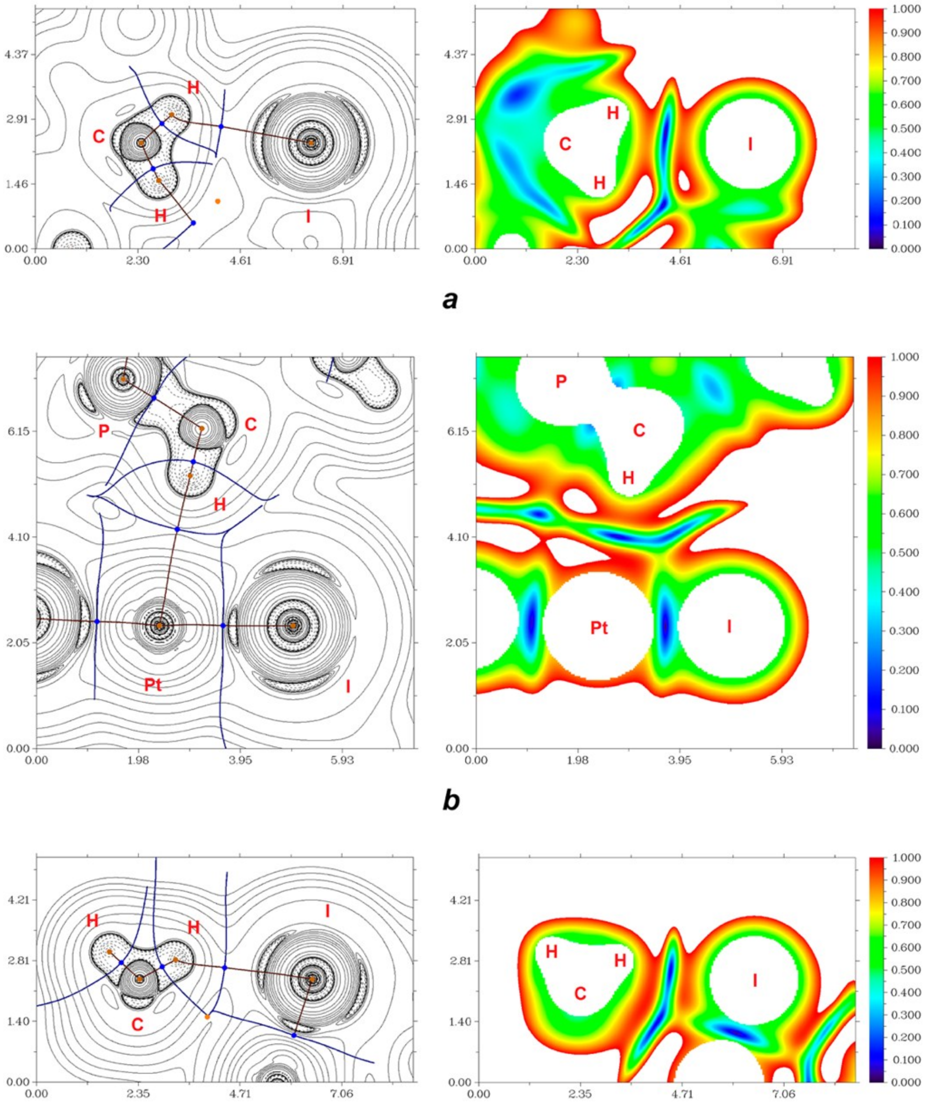

a

b

c

Fig. S13. Contour line diagram of the Laplacian distribution $\nabla^2\rho(\mathbf{r})$, bond paths and selected zero-flux surfaces (left) and RDG isosurface (right) referring to: (*a*) C5–H5A•••I3–Pt1 HB in $[n\mathrm{Bu_4N}]^+{}_2[\mathrm{Pt_2}(\mu\text{-I})_2\mathrm{I_4}]^{2-}$•(1,4-FIB)$_4$; (*b*) C13–H13A•••Pt1 HB in $[n\mathrm{Bu_4P}]^+{}_2[\mathrm{Pt_2}(\mu\text{-I})_2\mathrm{I_4}]^{2-}$•$(\mathrm{C_2I_4})_4$; (*c*) C24–H24C•••I6–Pt2 HB in $[n\mathrm{Bu_4P}]^+{}_2[\mathrm{Pt_2}(\mu\text{-I})_2\mathrm{I_4}]^{2-}$•$(\mathrm{C_2I_4})_4$. Bond critical points (3, –1) are shown in blue, nuclear critical points (3, –3) – in pale brown, ring critical points (3, +1) – in orange. Length units – Å, RDG isosurface values are given in a.u.

Table S10. Cartesian atomic coordinates for model clusters.

Atom	X	Y	Z
$[Pt_2(\mu\text{-}I)_2I_4]^{2-}$•(1,3,5-FIB)$_5$			
Pt	0.864961	-0.492640	14.338222
Pt	0.170257	-1.153420	18.033507
I	1.262889	1.636892	12.893737
I	0.696895	-1.998741	12.226093
I	-0.418406	-3.294696	19.408755
I	0.859983	0.868501	16.544711
I	0.479198	-2.554681	15.871132
I	-0.111852	0.433167	20.077190
I	-3.565655	9.104465	10.505649
I	-0.725091	4.482438	13.246847
I	-4.093075	8.266556	16.487541
F	-4.417977	9.473128	13.540610
F	-1.623534	6.625317	11.059151
F	-2.287251	5.846239	15.624252
C	-3.334084	7.706156	14.640689
C	-3.049645	8.068737	12.258931
C	-1.942330	6.185309	13.329140
C	-3.592575	8.421816	13.475527
C	-2.517954	6.590959	14.520019
C	-2.216022	6.966803	12.217389
I	2.426329	-5.180789	27.047986
I	-1.320015	-0.990678	29.323514
I	0.204278	-0.871916	23.451017
F	0.730200	-3.407347	29.089888
F	-1.162359	-0.177147	26.249978
F	1.773623	-3.397378	24.533886
C	-0.247102	-1.771017	27.720575
C	0.575518	-2.880875	27.863006
C	0.328066	-1.756591	25.342774
C	1.256348	-3.465974	26.812580
C	-0.358646	-1.238366	26.436721
C	1.107187	-2.866359	25.572246
I	2.686924	-4.918104	12.516098
I	6.433268	-9.108215	10.240570
I	4.908974	-9.226977	16.113067
F	4.383052	-6.691545	10.474196
F	6.275612	-9.921746	13.314106
F	3.339629	-6.701514	15.030198
C	5.360355	-8.327875	11.843509
C	4.537735	-7.218018	11.701078

C	4.785186	-8.342302	14.221310
C	3.856905	-6.632918	12.751504
C	5.471899	-8.860526	13.127363
C	4.006066	-7.232533	13.991838
I	-0.303021	-0.212329	9.276393
I	-3.143585	4.409698	6.535195
I	0.224400	0.625580	3.294501
F	0.549302	-0.580992	6.241432
F	-2.245141	2.266819	8.722891
F	-1.581424	3.045898	4.157790
C	-0.534592	1.185981	5.141353
C	-0.819030	0.823399	7.523111
C	-1.926346	2.706827	6.452902
C	-0.276100	0.470321	6.306515
C	-1.350721	2.301177	5.262023
C	-1.652653	1.925333	7.564653
I	6.791206	-5.261775	29.058435
I	3.950642	-0.639748	26.317237
I	7.318626	-4.423866	23.076543
F	7.643529	-5.630438	26.023474
F	4.849085	-2.782627	28.504933
F	5.512802	-2.003548	23.939832
C	6.559635	-3.863466	24.923395
C	6.275197	-4.226047	27.305153
C	5.167881	-2.342619	26.234944
C	6.818126	-4.579125	26.088557
C	5.743505	-2.748269	25.044065
C	5.441573	-3.124113	27.346695
$[Pt_2(\mu\text{-}I)_2I_4]^{2-}$•$(IPFB)_2$			
Pt	1.889211	4.568878	17.613545
I	4.090775	5.027605	16.315811
I	0.628226	3.768453	15.484888
I	3.052912	5.279656	19.822921
Pt	0.926347	5.006753	21.287345
I	-1.275217	4.548026	22.585078
I	2.187332	5.807178	23.416001
I	-0.237355	4.295975	19.077969
I	4.435253	4.658034	12.885725
F	6.120170	3.380484	7.048841
F	5.461853	6.532600	10.470174
F	6.220062	5.964883	7.951342
F	4.423481	1.986595	11.160665
F	5.188580	1.426767	8.635997
C	5.711067	3.667149	8.285889

C	4.934134	4.278272	10.880579
C	4.859441	2.979335	10.390428
C	5.383278	5.266605	10.036429
C	5.780255	4.976123	8.719634
C	5.253688	2.692977	9.096973
I	-1.619696	4.917597	26.015164
F	-3.304612	6.195146	31.852048
F	-2.646295	3.043031	28.430715
F	-3.404504	3.610748	30.949548
F	-1.607923	7.589036	27.740224
F	-2.373023	8.148864	30.264892
C	-2.895509	5.908482	30.615000
C	-2.118576	5.297359	28.020311
C	-2.043883	6.596295	28.510462
C	-2.567720	4.309026	28.864460
C	-2.964697	4.599507	30.181255
C	-2.438130	6.882653	29.803916
$[n\mathrm{Bu_4N}]^{+}{}_2[\mathrm{Pt_2}(\mu\text{-I})_2\mathrm{I_4}]^{2-}\bullet(1{,}4\text{-FIB})_4$			
Pt	1.922548	4.493635	1.685709
I	0.991651	2.876535	-0.115109
I	2.570393	6.237664	3.500779
I	3.007961	2.522895	2.989548
Pt	0.106312	4.743375	-1.685709
I	1.037210	6.360476	0.115109
I	-0.541533	2.999346	-3.500779
I	-0.979101	6.714115	-2.989548
I	1.819553	4.678022	6.572730
I	-0.010474	1.895678	12.727048
F	2.255421	1.147949	10.617445
F	-0.325945	5.553894	8.790134
F	-1.021213	4.510543	11.136715
F	2.974899	2.197026	8.293520
C	1.337365	3.901889	8.454125
C	0.595987	2.798100	10.946328
C	1.982964	2.794646	8.973029
C	0.332741	4.461096	9.221519
C	1.617306	2.244465	10.186243
C	-0.031450	3.922744	10.447522
N	7.112541	4.996086	4.040695
C	7.995081	3.817081	3.641468
H	8.703706	4.148652	3.067749
H	8.412214	3.465191	4.441750
C	6.142198	4.587700	5.137155
H	5.501119	5.305990	5.254822

H	5.650631	3.809707	4.830928
C	7.302121	2.672456	2.925233
H	6.426340	2.523716	3.314411
H	7.183392	2.895621	1.987916
C	7.012733	5.903873	1.646243
H	7.395696	5.126647	1.211386
H	7.736480	6.501123	1.891078
C	8.041109	6.074558	4.533106
H	8.683747	6.267751	3.833316
H	8.535942	5.727585	5.293192
C	8.136099	1.419502	3.049478
H	8.198623	1.172082	3.984968
H	9.033020	1.603165	2.729730
C	6.259294	5.476663	2.888690
H	5.725309	6.225878	3.193821
H	5.647657	4.764874	2.643855
C	6.742708	4.263118	6.493615
H	7.163794	5.053484	6.866350
H	7.418871	3.573887	6.400432
C	7.388397	7.374986	4.949692
H	6.653584	7.193651	5.556298
H	7.031768	7.826248	4.167681
C	5.628189	3.778277	7.421797
H	4.939290	4.459254	7.472956
H	5.227479	2.978437	7.047235
C	6.051304	6.622469	0.676038
H	6.479239	6.704368	-0.190021
H	5.254479	6.081178	0.562756
C	5.645759	8.002842	1.160227
H	5.060662	8.408487	0.517077
H	6.429754	8.547112	1.268027
H	5.191253	7.926157	2.002533
C	7.561890	0.255211	2.267467
H	7.634305	0.433562	1.326495
H	6.637851	0.137934	2.501339
H	8.049412	-0.543847	2.479414
C	8.414249	8.267082	5.634865
H	9.190468	8.358491	5.061147
H	8.702520	7.844396	6.458900
C	6.129379	3.472730	8.825032
H	6.776278	2.764549	8.784835
H	5.391109	3.200872	9.374997
H	6.535348	4.258477	9.197766
C	7.859893	9.660177	5.954612

H	7.530407	10.065849	5.148849
H	8.558985	10.206208	6.323692
H	7.144842	9.582416	6.590453
N	-5.083680	4.240924	-4.040695
C	-5.966220	5.419930	-3.641468
H	-6.674846	5.088359	-3.067749
H	-6.383353	5.771819	-4.441750
C	-4.113338	4.649310	-5.137155
H	-3.472258	3.931021	-5.254822
H	-3.621771	5.427303	-4.830928
C	-5.273260	6.564554	-2.925233
H	-4.397479	6.713294	-3.314411
H	-5.154531	6.341389	-1.987916
C	-4.983873	3.333138	-1.646243
H	-5.366836	4.110364	-1.211386
H	-5.707619	2.735887	-1.891078
C	-6.012248	3.162452	-4.533106
H	-6.654887	2.969259	-3.833316
H	-6.507082	3.509425	-5.293192
C	-6.107238	7.817508	-3.049478
H	-6.169763	8.064928	-3.984968
H	-7.004160	7.633845	-2.729730
C	-4.230433	3.760347	-2.888690
H	-3.696449	3.011132	-3.193821
H	-3.618797	4.472137	-2.643855
C	-4.713848	4.973892	-6.493615
H	-5.134934	4.183526	-6.866350
H	-5.390010	5.663123	-6.400432
C	-5.359536	1.862024	-4.949692
H	-4.624724	2.043359	-5.556298
H	-5.002908	1.410762	-4.167681
C	-3.599328	5.458733	-7.421797
H	-2.910429	4.777756	-7.472956
H	-3.198619	6.258574	-7.047235
C	-4.022444	2.614541	-0.676038
H	-4.450378	2.532642	0.190021
H	-3.225619	3.155832	-0.562756
C	-3.616898	1.234168	-1.160227
H	-3.031801	0.828523	-0.517077
H	-4.400894	0.689898	-1.268027
H	-3.162392	1.310853	-2.002533
C	-5.533030	8.981799	-2.267467
H	-5.605444	8.803448	-1.326495
H	-4.608991	9.099076	-2.501339

H	-6.020552	9.780857	-2.479414
C	-6.385388	0.969928	-5.634865
H	-7.161608	0.878519	-5.061147
H	-6.673660	1.392614	-6.458900
C	-4.100519	5.764280	-8.825032
H	-4.747418	6.472461	-8.784835
H	-3.362249	6.036138	-9.374997
H	-4.506488	4.978533	-9.197766
C	-5.831033	-0.423167	-5.954612
H	-5.501547	-0.828839	-5.148849
H	-6.530125	-0.969198	-6.323692
H	-5.115982	-0.345406	-6.590453
I	0.209307	4.558988	-6.572730
I	2.039334	7.341333	-12.727048
F	-0.226561	8.089062	-10.617445
F	2.354806	3.683116	-8.790134
F	3.050074	4.726467	-11.136715
F	-0.946038	7.039984	-8.293520
C	0.691495	5.335121	-8.454125
C	1.432874	6.438910	-10.946328
C	0.045896	6.442364	-8.973029
C	1.696119	4.775914	-9.221519
C	0.411555	6.992545	-10.186243
C	2.060310	5.314266	-10.447522
I	2.254155	11.531037	-11.698557
I	0.424128	8.748693	-5.544239
F	2.690023	8.000963	-7.653842
F	0.108657	12.406909	-9.481154
F	-0.586611	11.363558	-7.134572
F	3.409501	9.050041	-9.977767
C	1.771967	10.754904	-9.817163
C	1.030589	9.651115	-7.324959
C	2.417566	9.647661	-9.298258
C	0.767343	11.314111	-9.049768
C	2.051908	9.097480	-8.085045
C	0.403152	10.775759	-7.823765
I	-0.225295	-2.294027	11.698557
I	1.604732	0.488318	5.544239
F	-0.661163	1.236047	7.653842
F	1.920204	-3.169899	9.481154
F	2.615472	-2.126548	7.134572
F	-1.380640	0.186969	9.977767
C	0.256893	-1.517893	9.817163
C	0.998272	-0.414105	7.324959

C	-0.388706	-0.410651	9.298258
C	1.261517	-2.077101	9.049768
C	-0.023047	0.139530	8.085045
C	1.625708	-1.538749	7.823765
$[n\mathrm{Bu}_4\mathrm{P}]^+{}_2[\mathrm{Pt}_2(\mu\text{-I})_2\mathrm{I}_4]^{2-}\bullet(\mathrm{C}_2\mathrm{I}_4)_4$			
Pt	-0.449791	15.573790	17.960076
Pt	1.655458	15.552353	14.755095
I	-1.308810	17.464426	19.510959
I	0.567235	17.313210	16.317274
I	0.575004	13.808254	16.350276
I	2.663200	17.415756	13.241866
I	2.663387	13.660725	13.291923
I	-1.413403	13.735795	19.521148
I	4.264048	7.891602	15.454344
I	7.035625	11.442847	17.829839
I	4.373972	11.530758	15.481365
I	6.902231	7.798685	17.858855
C	5.578718	9.032093	16.700454
C	5.632336	10.282777	16.700454
I	-6.367052	7.891602	15.454344
I	-3.595475	11.442847	17.829839
I	-6.257128	11.530758	15.481365
I	-3.728869	7.798685	17.858855
C	-5.052382	9.032093	16.700454
C	-4.998764	10.282777	16.700454
I	-6.222685	19.657217	15.454344
I	-3.451107	23.208461	17.829839
I	-6.112760	23.296372	15.481365
I	-3.584502	19.564300	17.858855
C	-4.908015	20.797707	16.700454
C	-4.854397	22.048392	16.700454
I	4.408415	19.657217	15.454344
I	7.179993	23.208461	17.829839
I	4.518340	23.296372	15.481365
I	7.046598	19.564300	17.858855
C	5.723085	20.797707	16.700454
C	5.776703	22.048392	16.700454
P	1.908434	15.754985	8.495969
C	2.550069	17.412048	8.826212
H	2.943745	17.420342	9.734549
H	1.792344	18.048382	8.824219
C	4.230540	19.229757	8.232837
H	4.777549	19.565390	7.479766
H	3.506171	19.885866	8.392311

C	3.216773	14.558137	8.149999
H	3.769890	14.912535	7.408889
H	2.792685	13.723272	7.827507
C	0.785608	15.779288	7.089719
H	0.195522	16.568607	7.176323
H	0.212232	14.972792	7.134239
C	1.004337	15.221707	9.940093
H	1.580145	15.334989	10.737905
H	0.799132	14.258112	9.851939
C	3.608638	17.912182	7.831273
H	3.188376	18.013661	6.939327
H	4.322658	17.230633	7.752200
C	-0.304684	15.989535	10.162027
H	-0.157287	16.949481	9.971544
H	-0.990194	15.654132	9.530777
C	1.448245	15.822060	5.707391
H	1.968575	14.990605	5.572725
H	2.080094	16.583765	5.674611
C	4.152964	14.198986	9.319252
H	4.654563	13.380996	9.076719
H	3.595311	13.982067	10.108869
C	0.437932	15.964935	4.578228
H	-0.074320	16.802456	4.702263
H	-0.200095	15.209360	4.613667
C	5.151449	15.266202	9.723474
H	5.612996	15.607256	8.915030
H	4.671206	16.022972	10.142093
C	1.115208	15.988616	3.218271
H	1.754247	16.731455	3.185047
H	1.589218	15.143351	3.074301
H	0.439475	16.106840	2.518358
C	-0.821566	15.830725	11.599507
H	-1.672195	16.328856	11.692533
H	-0.166419	16.238248	12.221897
C	-1.051854	14.387468	12.007051
H	-1.402521	14.357535	12.921810
H	-1.696986	13.973919	11.395734
H	-0.203949	13.896651	11.967182
C	6.182536	14.714957	10.700251
H	5.726969	14.375429	11.499835
H	6.679815	13.985804	10.274988
H	6.804039	15.428400	10.957181
C	5.104628	19.159823	9.475404
H	4.561228	18.885642	10.243979

H	5.822423	18.506545	9.333649
H	5.495777	20.042102	9.650382
P	4.218382	15.730347	19.178722
C	3.750150	13.986724	19.248492
H	3.282441	13.757492	18.405938
H	4.577532	13.444024	19.283044
C	5.859738	15.396871	15.410045
H	5.823520	16.342520	15.116791
H	5.065975	14.935383	15.041483
C	5.806944	15.345034	16.922167
H	6.639186	15.732502	17.291836
H	5.752773	14.401636	17.214314
C	2.853114	13.571615	20.423282
H	3.283418	13.839282	21.274252
H	1.987261	14.045492	20.357278
C	2.605659	12.074927	20.434800
H	3.472582	11.599915	20.501247
H	2.174313	11.807302	19.584273
C	4.601638	16.115260	17.472352
H	3.809517	15.912466	16.913086
H	4.781112	17.085851	17.395937
C	5.690450	16.007002	20.170118
H	6.436099	15.494360	19.770326
H	5.927177	16.966718	20.115852
C	2.836246	16.734885	19.737102
H	2.008933	16.374473	19.329558
H	2.753520	16.626441	20.718309
C	7.111889	14.752888	14.851001
H	7.104901	14.819183	13.872009
H	7.139185	13.808969	15.112361
H	7.902735	15.212846	15.203172
C	6.789855	16.059858	22.463662
H	7.607688	15.787306	21.976380
H	6.787838	15.589287	23.334123
C	1.713846	11.664235	21.606490
H	0.821103	12.049781	21.489099
H	2.102778	11.991802	22.443727
H	1.646014	10.687260	21.639713
C	6.849927	17.561184	22.716162
H	6.909066	18.035555	21.861205
H	7.638238	17.768517	23.261031
H	6.041273	17.844468	23.192368
C	5.576364	15.614785	21.665849
H	4.763915	16.030616	22.049473

H	5.479529	14.632160	21.739385
C	3.258001	19.120233	21.796972
H	2.354611	19.472106	21.936512
H	3.905685	19.687418	22.264319
H	3.312061	18.206731	22.144714
C	2.905964	18.234299	19.427014
H	3.333125	18.331423	18.538833
H	1.975465	18.559968	19.336202
C	3.572818	19.113307	20.310765
H	3.417399	20.032756	19.976313
H	4.542297	18.935408	20.219953

S4. Characterization and spectra for 1–5

S4.1 NMR spectra

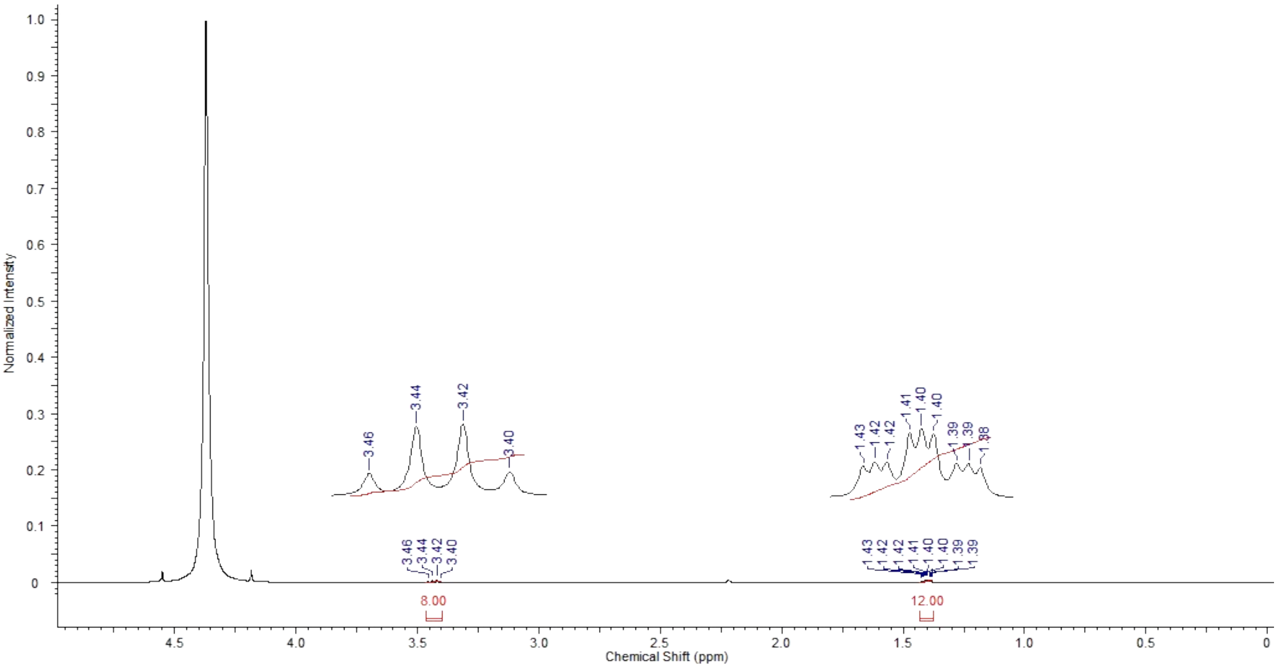

Fig. S14. ^{1}H NMR spectrum of **1** (MeNO$_2$, acetone-d_6; 298 K).

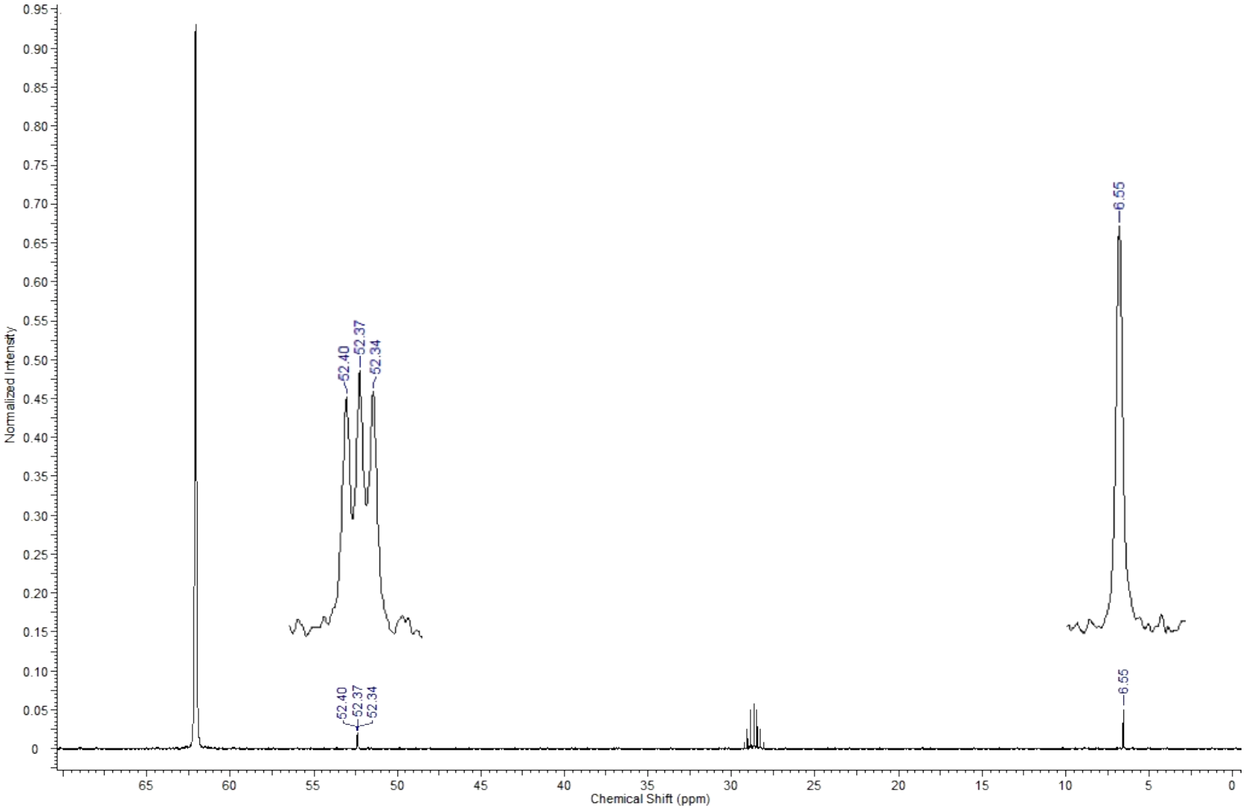

Fig. S15. $^{13}C\{^{1}H\}$ NMR spectrum of **1** (MeNO$_2$, acetone-d_6; 298 K).

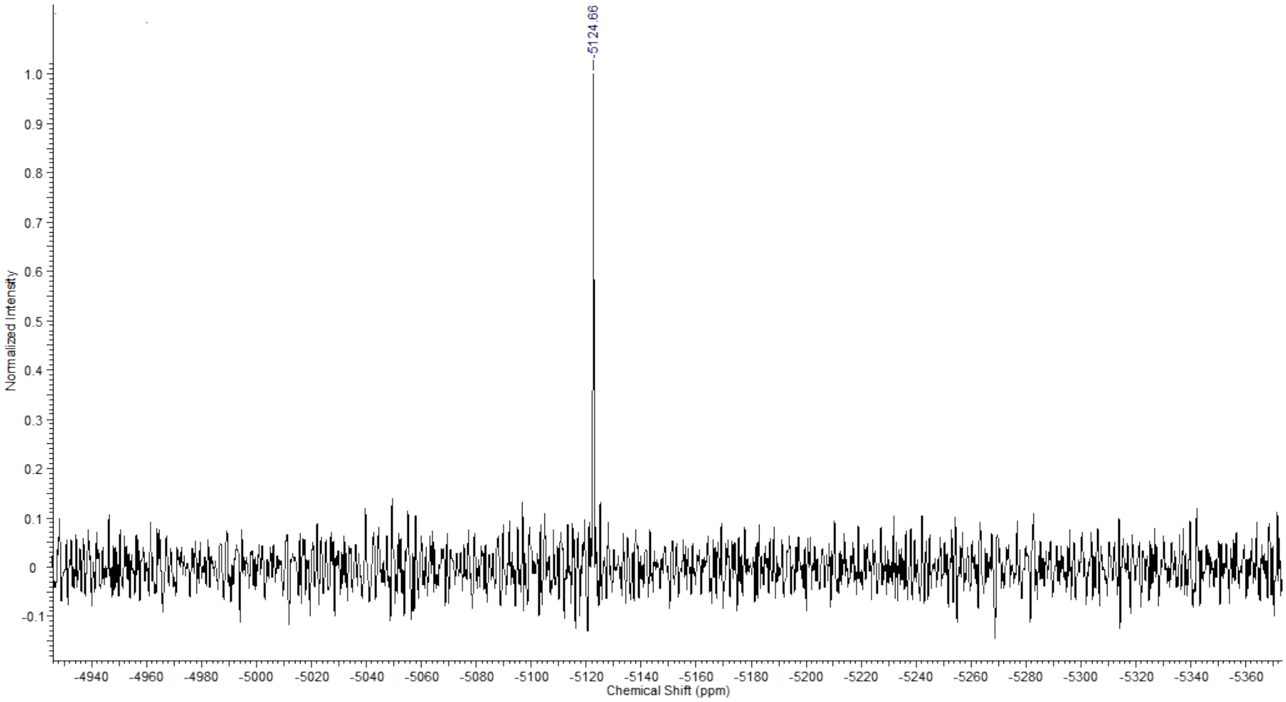

Fig. S16. ^{195}Pt NMR spectrum of **1** (MeNO$_2$, acetone-d_6; 298 K).

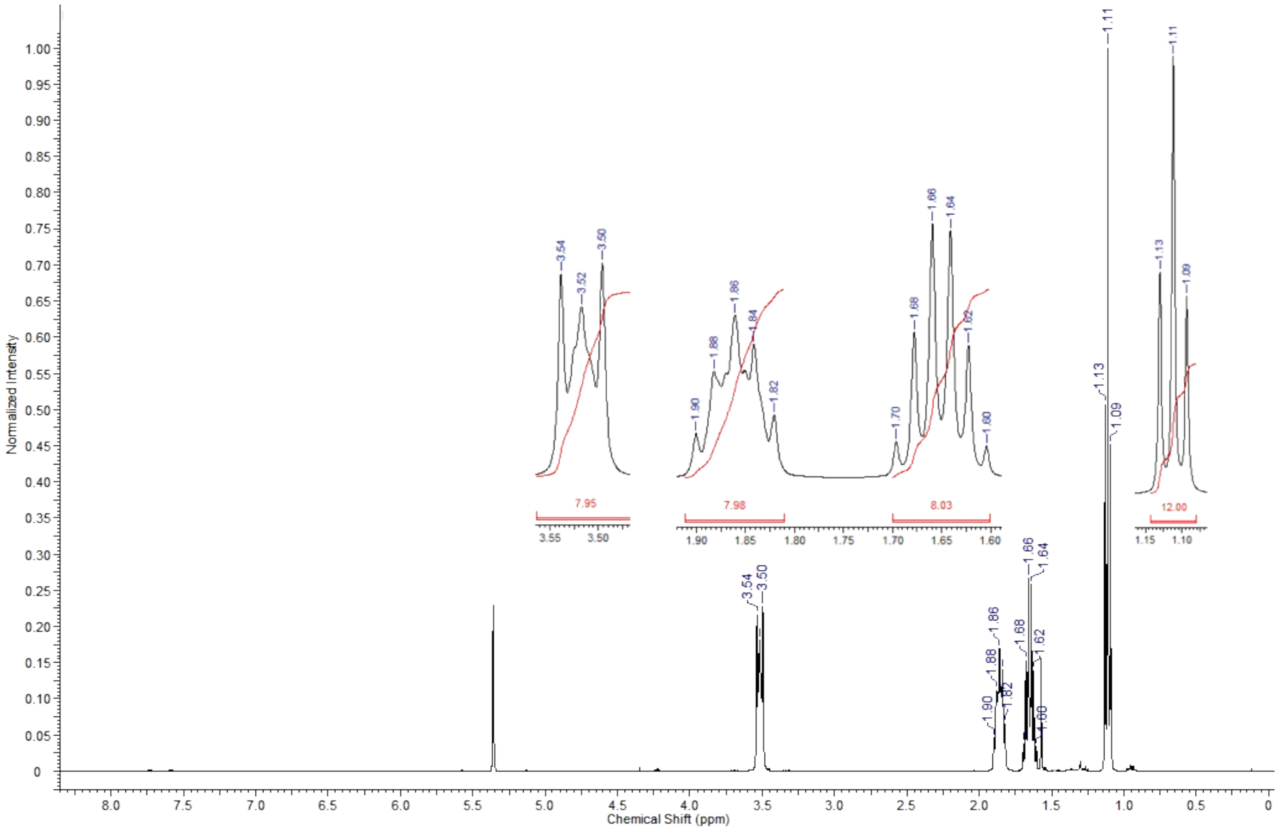

Fig. S17. ^{1}H NMR spectrum of **2** (CD$_2$Cl$_2$, 298 K).

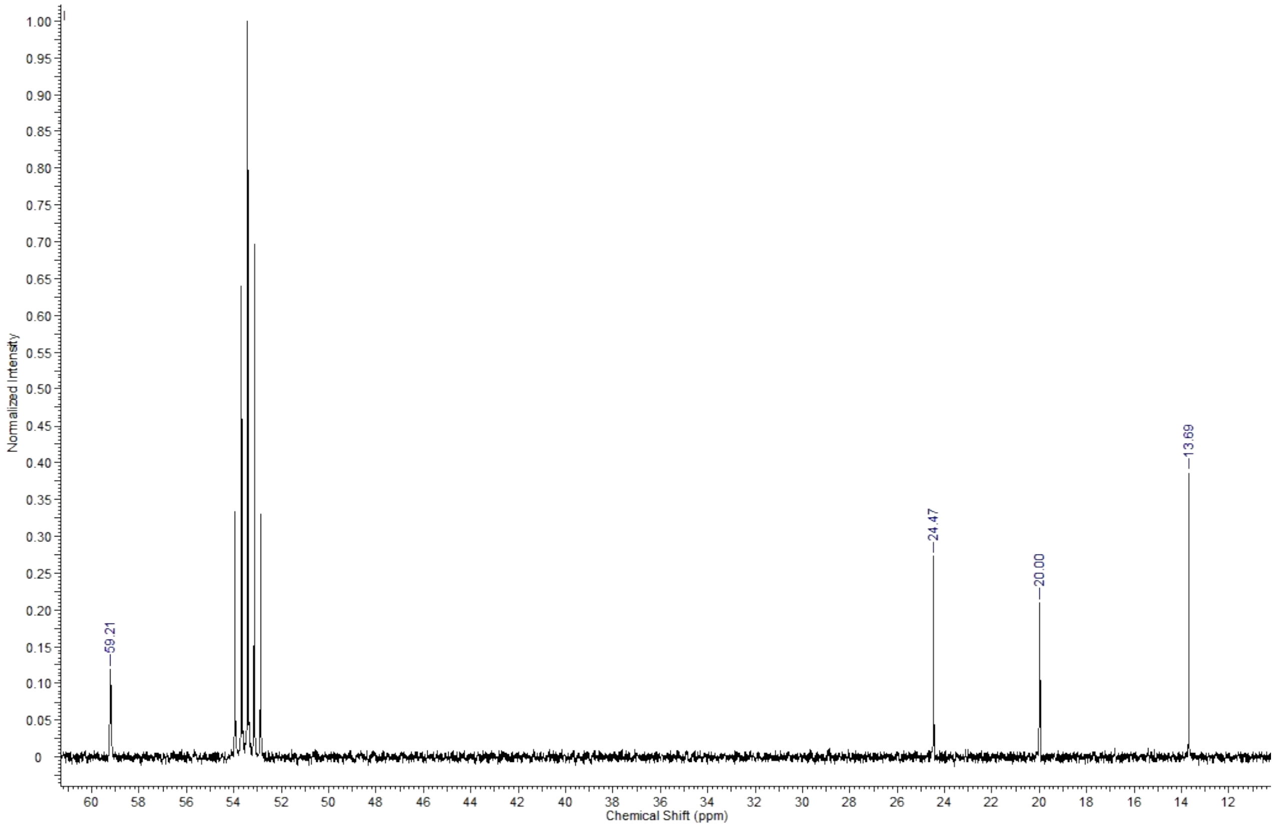

Fig. S18. $^{13}C\{^1H\}$ NMR spectrum of **2**(CD_2Cl_2, 298 K).

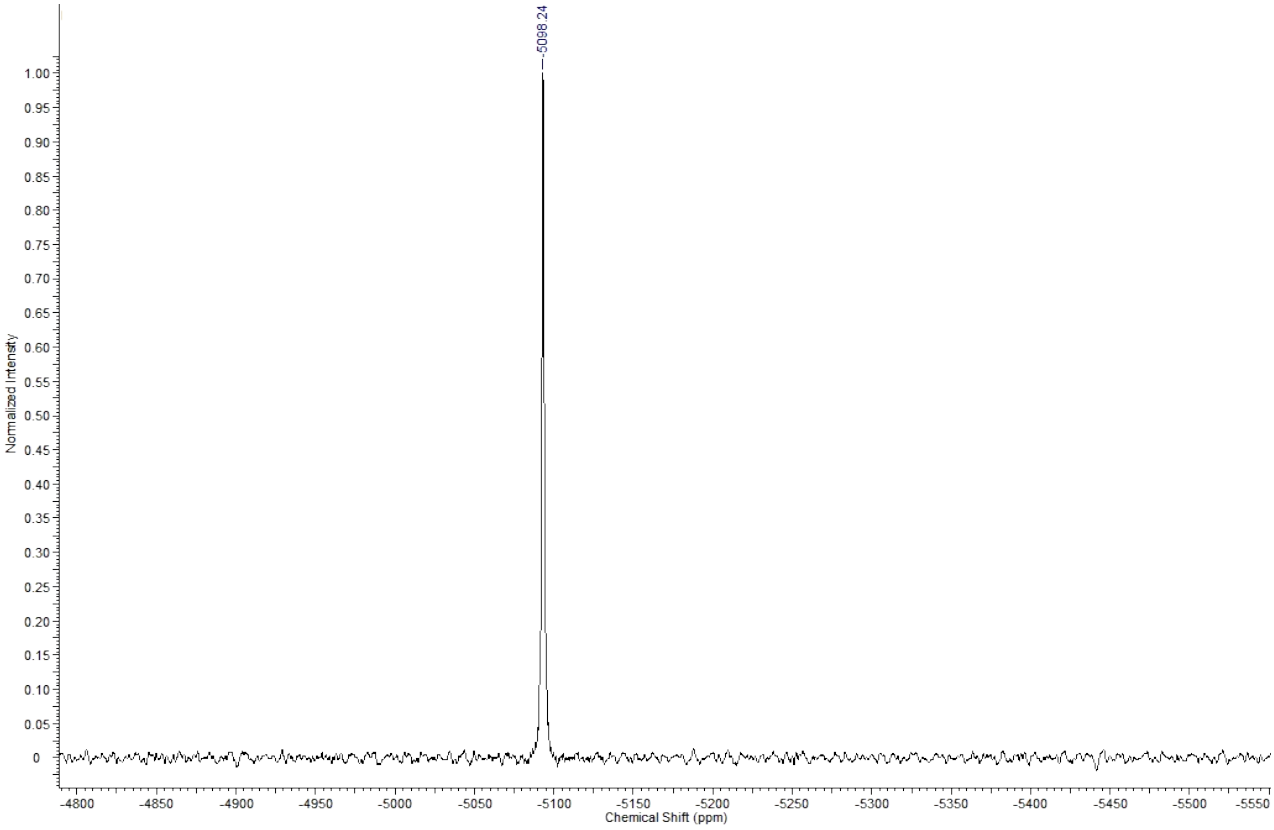

Fig. S19. ^{195}Pt NMR spectrum of **2** (CD_2Cl_2, 298 K).

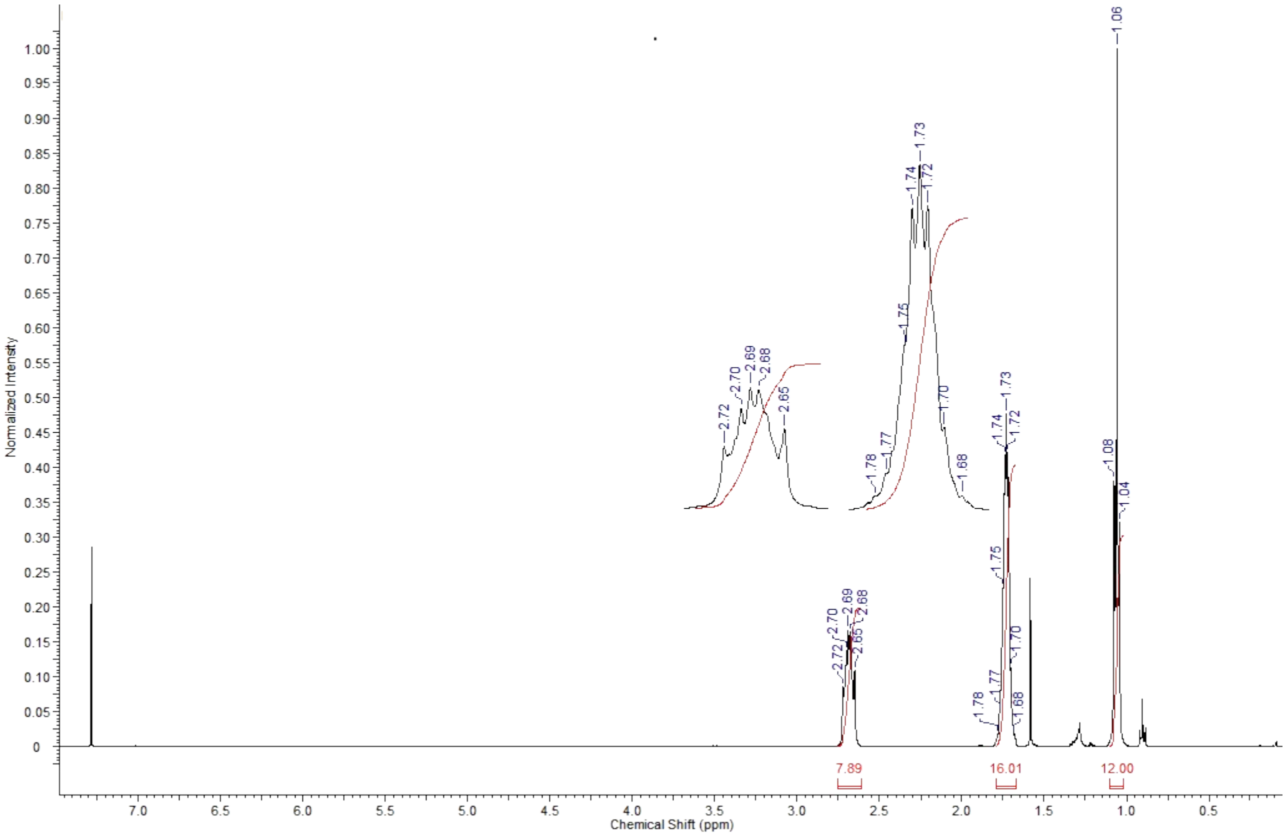

Fig. S20. ^{1}H NMR spectrum of **3** (CDCl$_3$, 298 K).

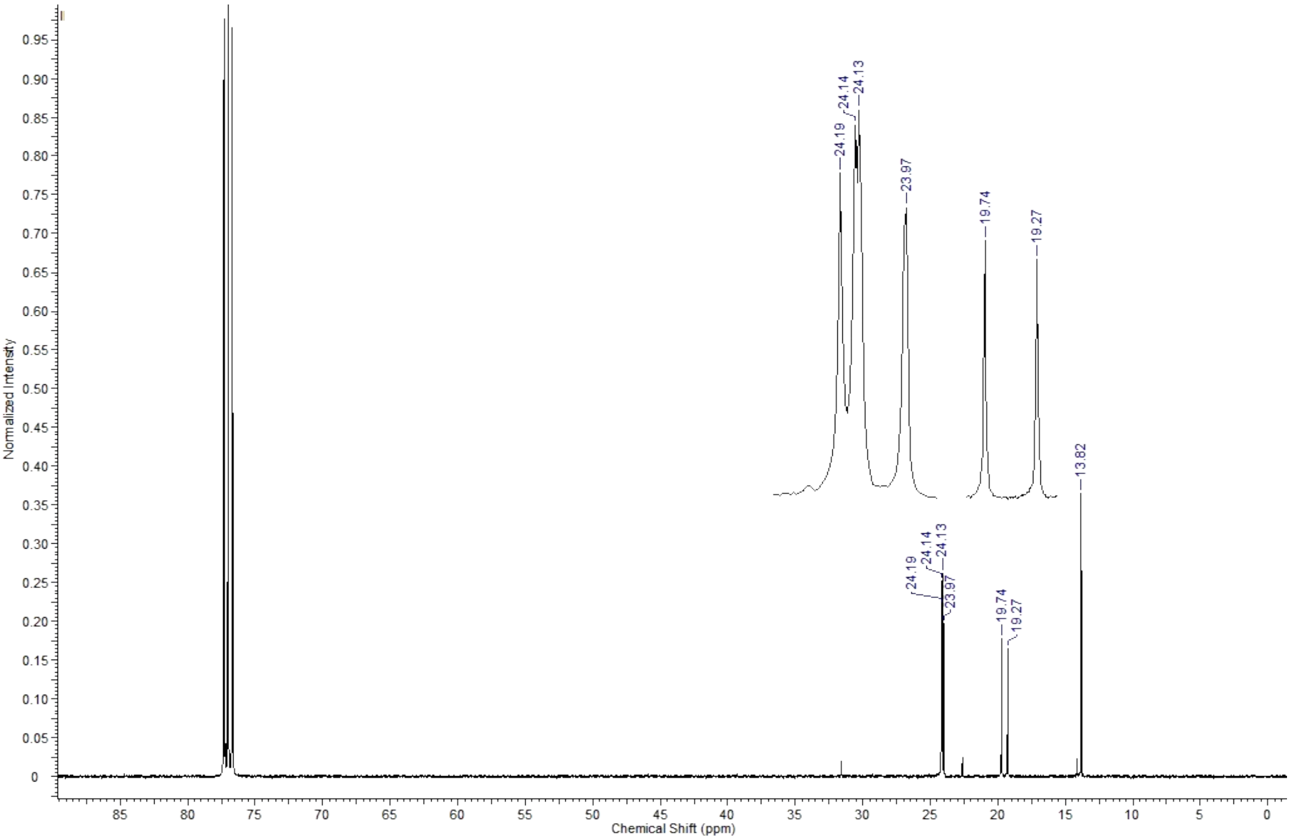

Fig. S21. ^{13}C{^{1}H} NMR spectrum of **3** (CDCl$_3$, 298 K).

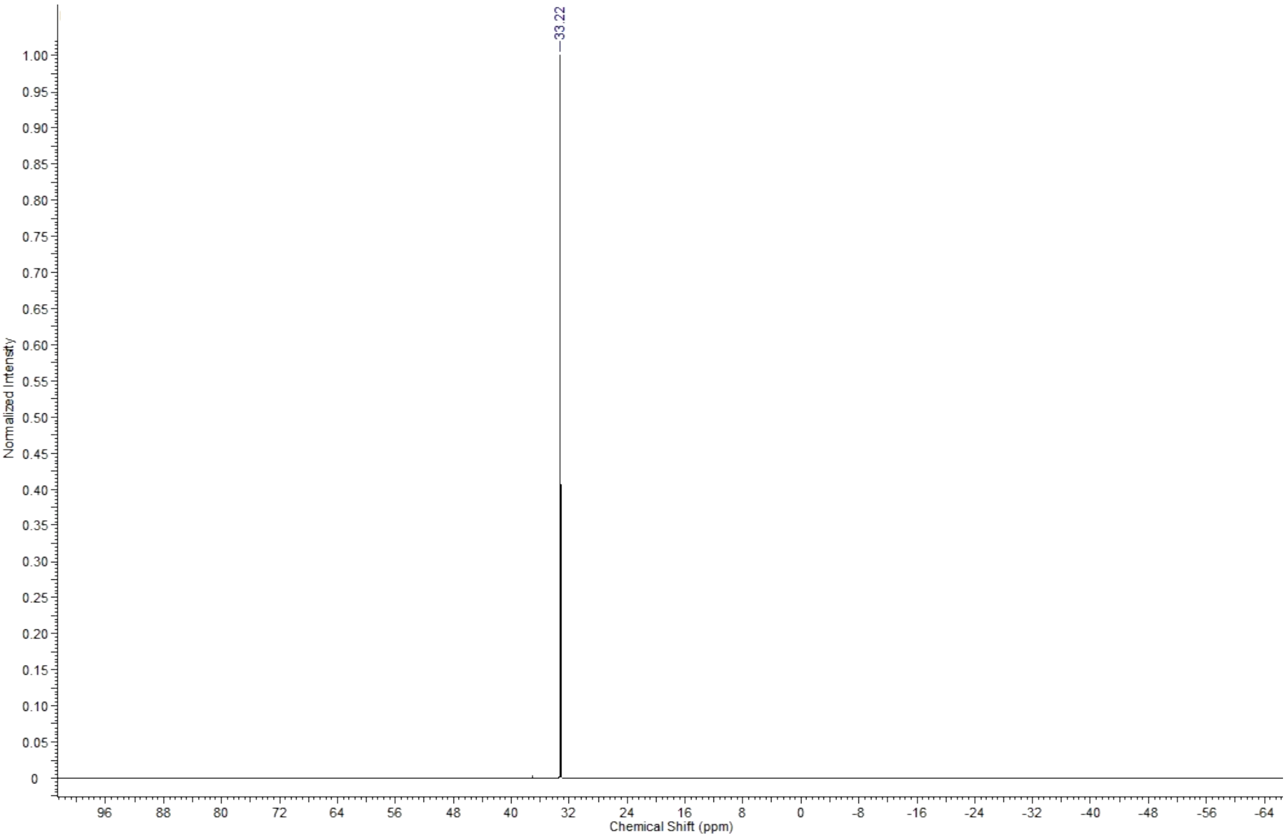

Fig. S22. ^{31}P NMR spectrum of **3** ($CDCl_3$, 298 K).

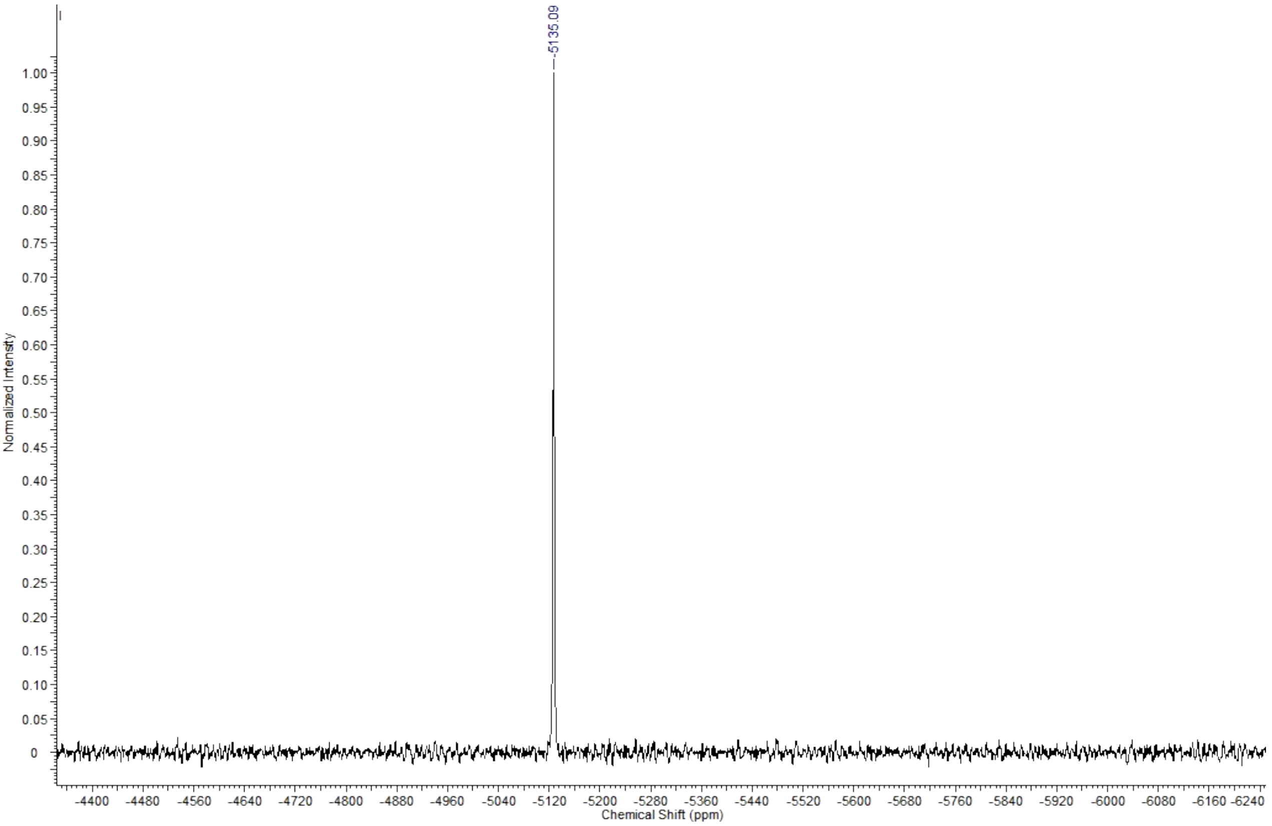

Fig. S23. ^{195}Pt NMR spectrum of **3** ($CDCl_3$, 298 K).

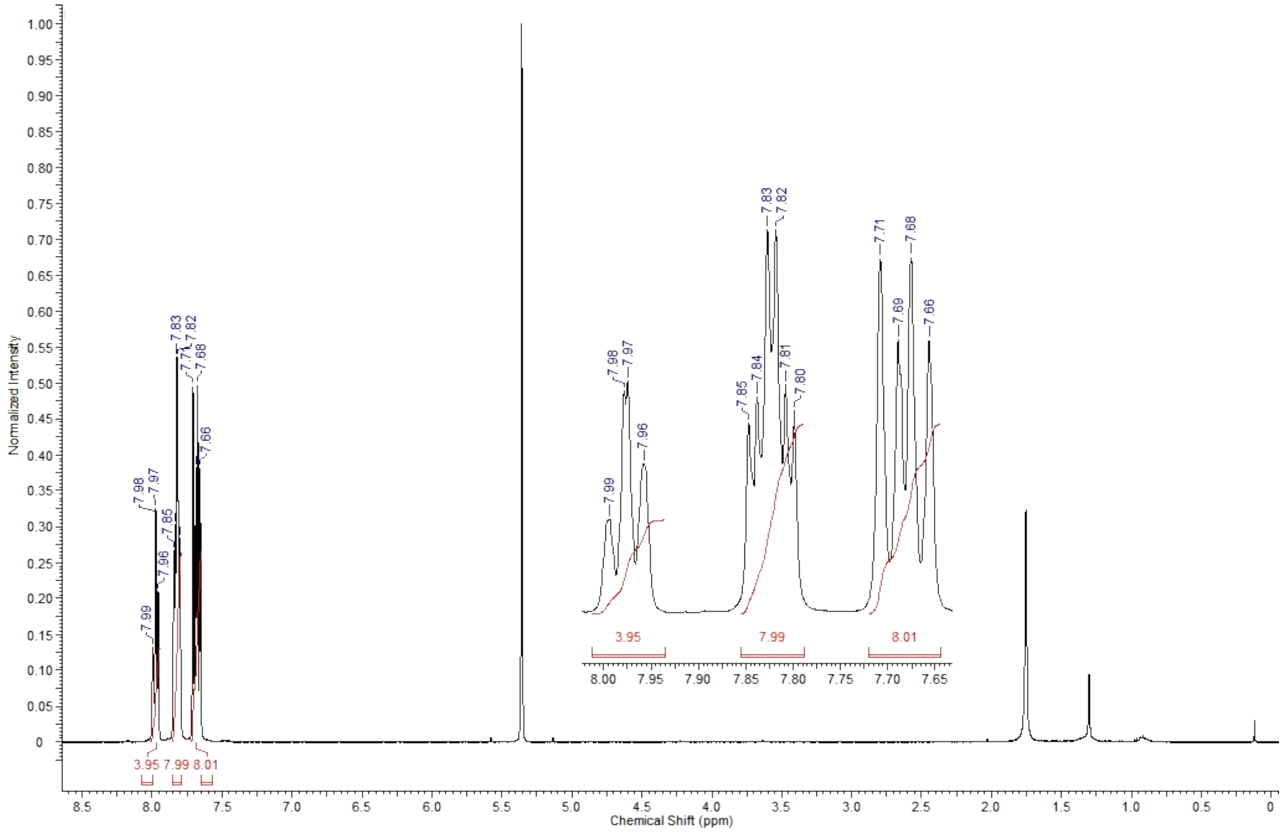

Fig. S24. ^{1}H NMR spectrum of **4** (CD_2Cl_2, 298 K).

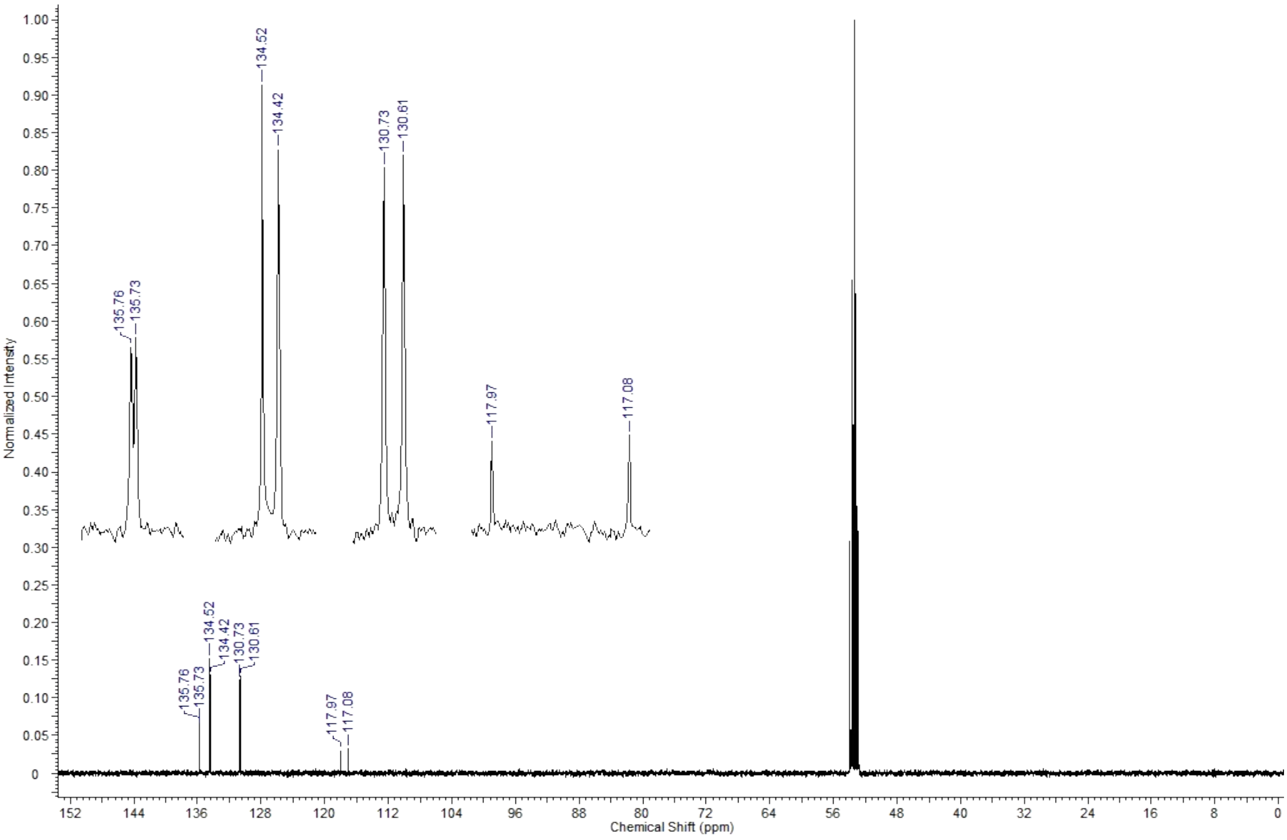

Fig. S25. $^{13}C\{^1H\}$ NMR spectrum of **4** (CD_2Cl_2, 298 K).

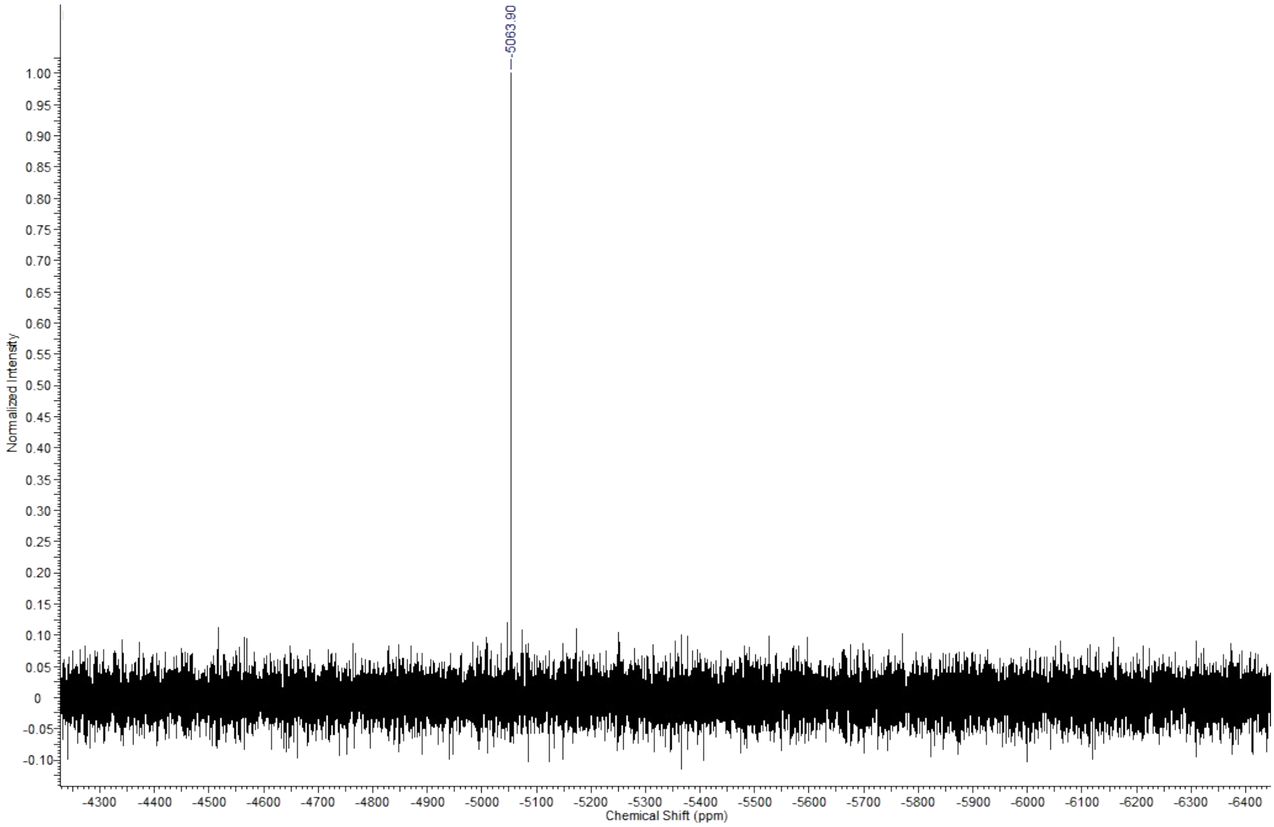

Fig. S26. ^{195}Pt NMR spectrum of **4** (CD_2Cl_2, 298 K).

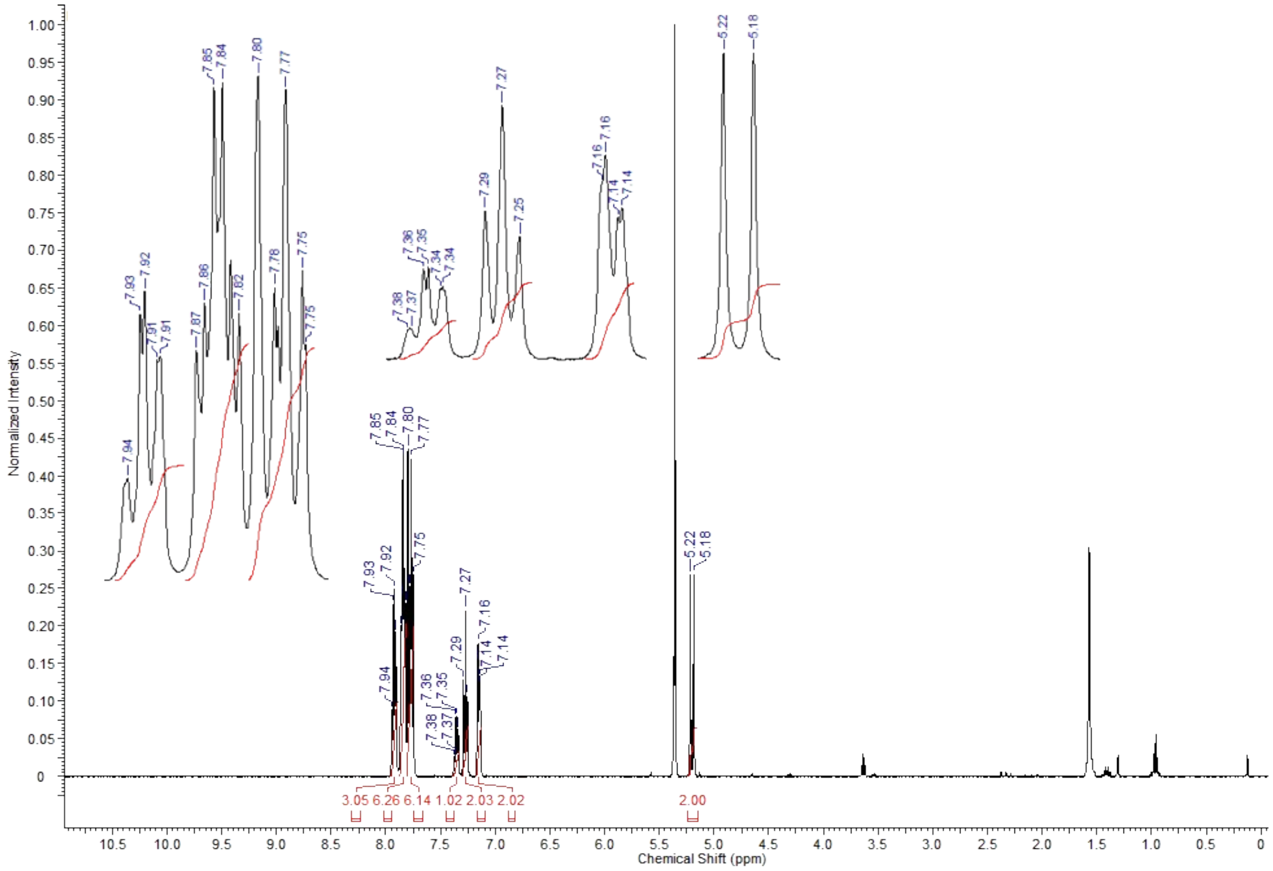

Fig. S27. ^{1}H NMR spectrum of **5** (CD_2Cl_2, 298 K).

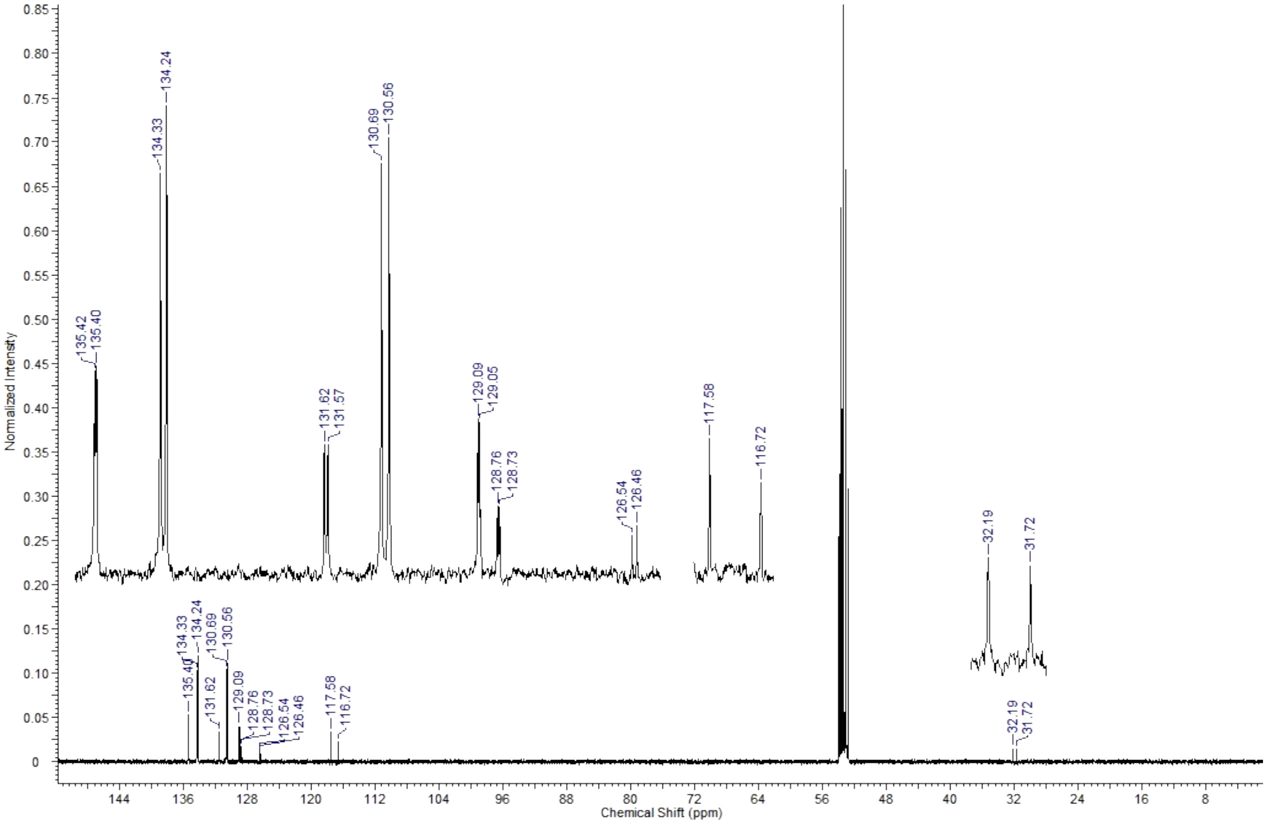

Fig. S28. $^{13}C\{^{1}H\}$ NMR spectrum of **5** (CD_2Cl_2, 298 K).

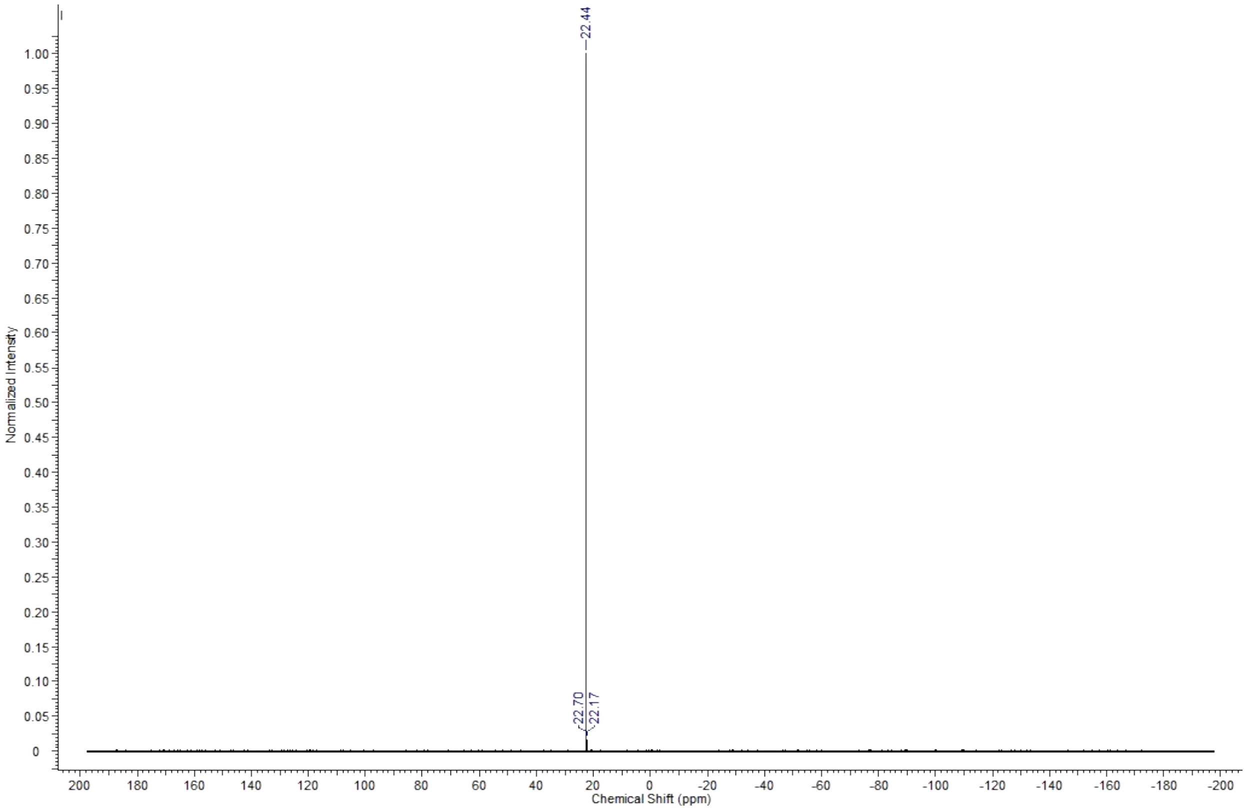

Fig. S29. ^{31}P NMR spectrum of **5** (CD_2Cl_2, 298 K).

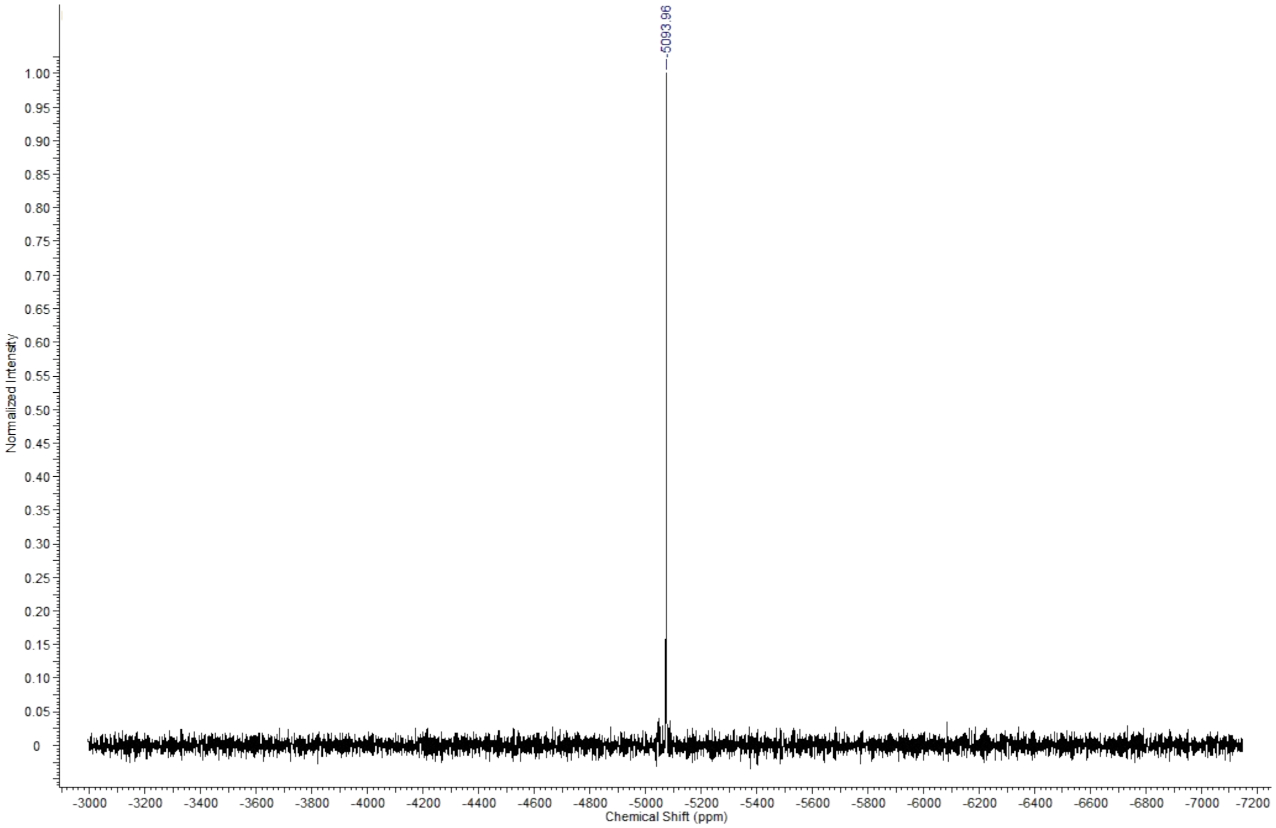

Fig. S30. ^{195}Pt NMR spectrum of **5** (CD_2Cl_2, 298 K).

S4.2 HRESI-MS

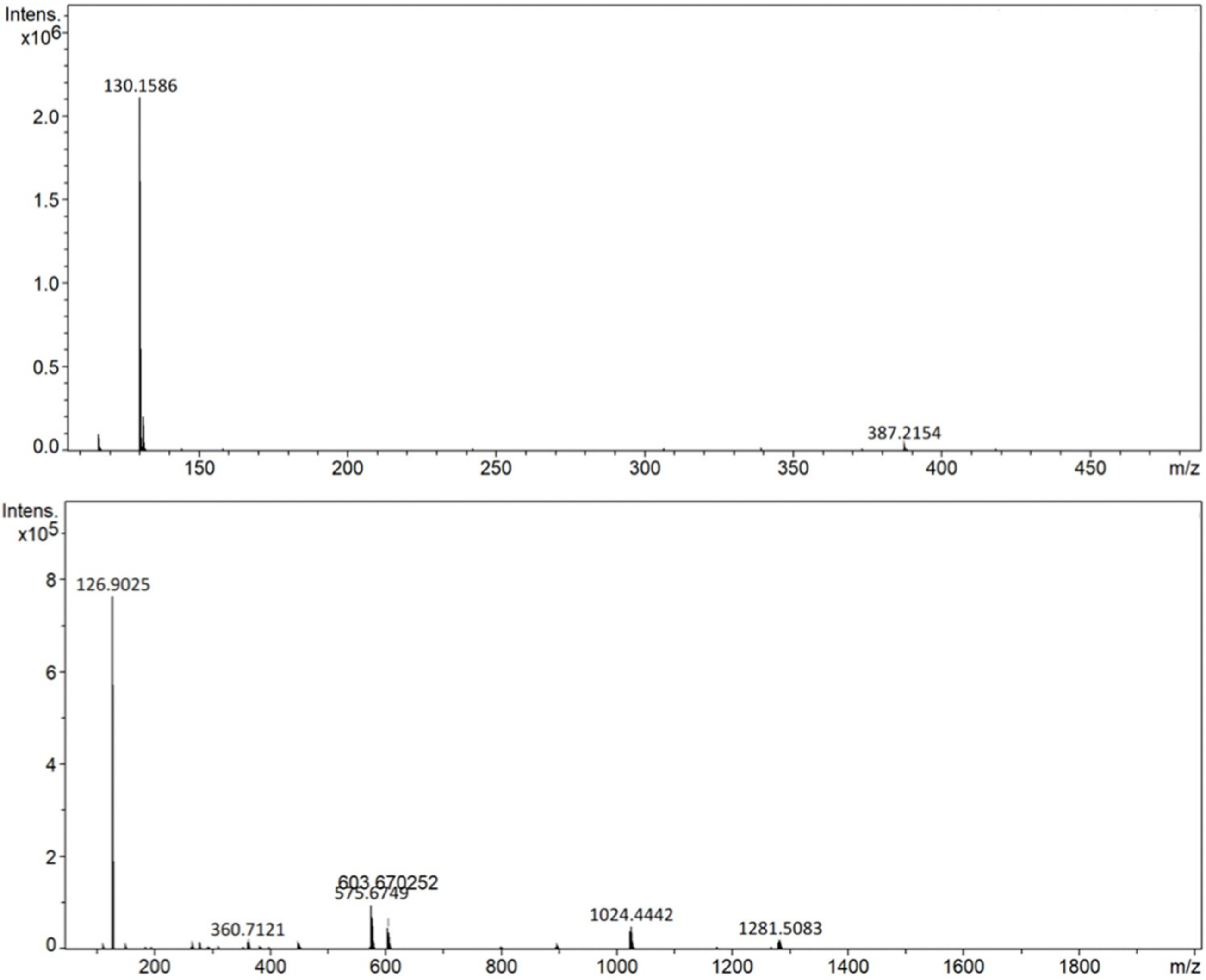

Fig. S31. Mass-spectra of **1**: *top* – HRESI$^+$-MS (calcd. for $[Et_4N]^+$ 130.1596, found 130.1586); *bottom* – HRESI$^–$-MS (calcd. for $[I]^–$ 126.9045, found 126.9025; calcd. for $[Pt_2I_6]^{2–}$ 575.6734, found 575.6749; calcd. for $[Pt_2I_5]^–$ 1024.4422, found 1024.4442; calcd. for $[M – Et_4N^+]^–$ 1281.5063, found 1281.5083).

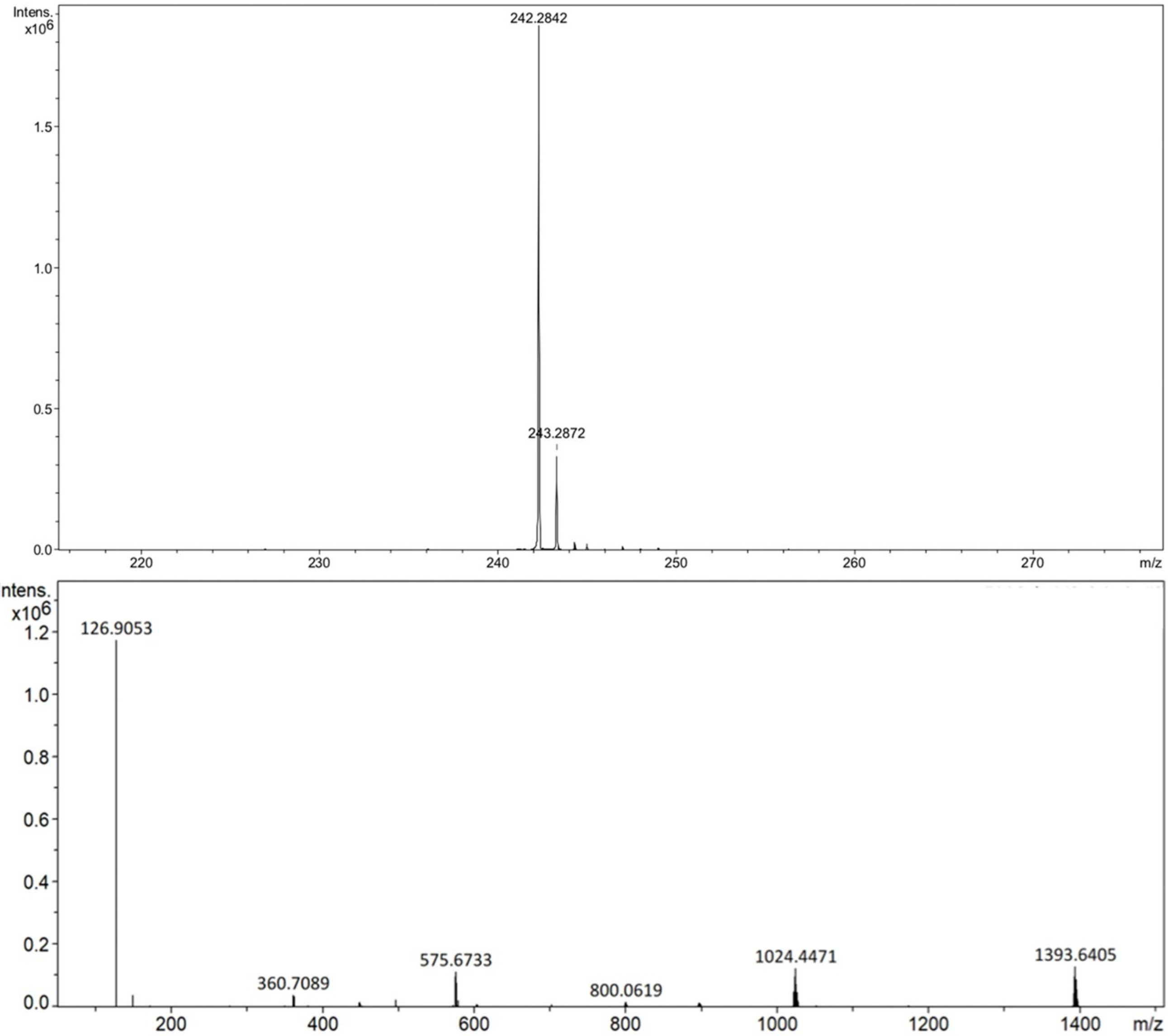

Fig. S32. Mass-spectra of **2**: *top* – HRESI$^+$-MS (calcd. for $[Bu_4N]^+$ 242.2848, found 242.2842); *bottom* – HRESI$^-$-MS (calcd. for $[I]^-$ 126.9045, found 126.9053; calcd. for $[Pt_2I_6]^{2-}$ 575.6734, found 575.6733; calcd. for calcd. for $[Pt_2I_5]^-$ 1024.4422, found 1024.4471; calcd. for $[M - Bu_4N^+]^-$ 1393.6315, found 1393.6405).

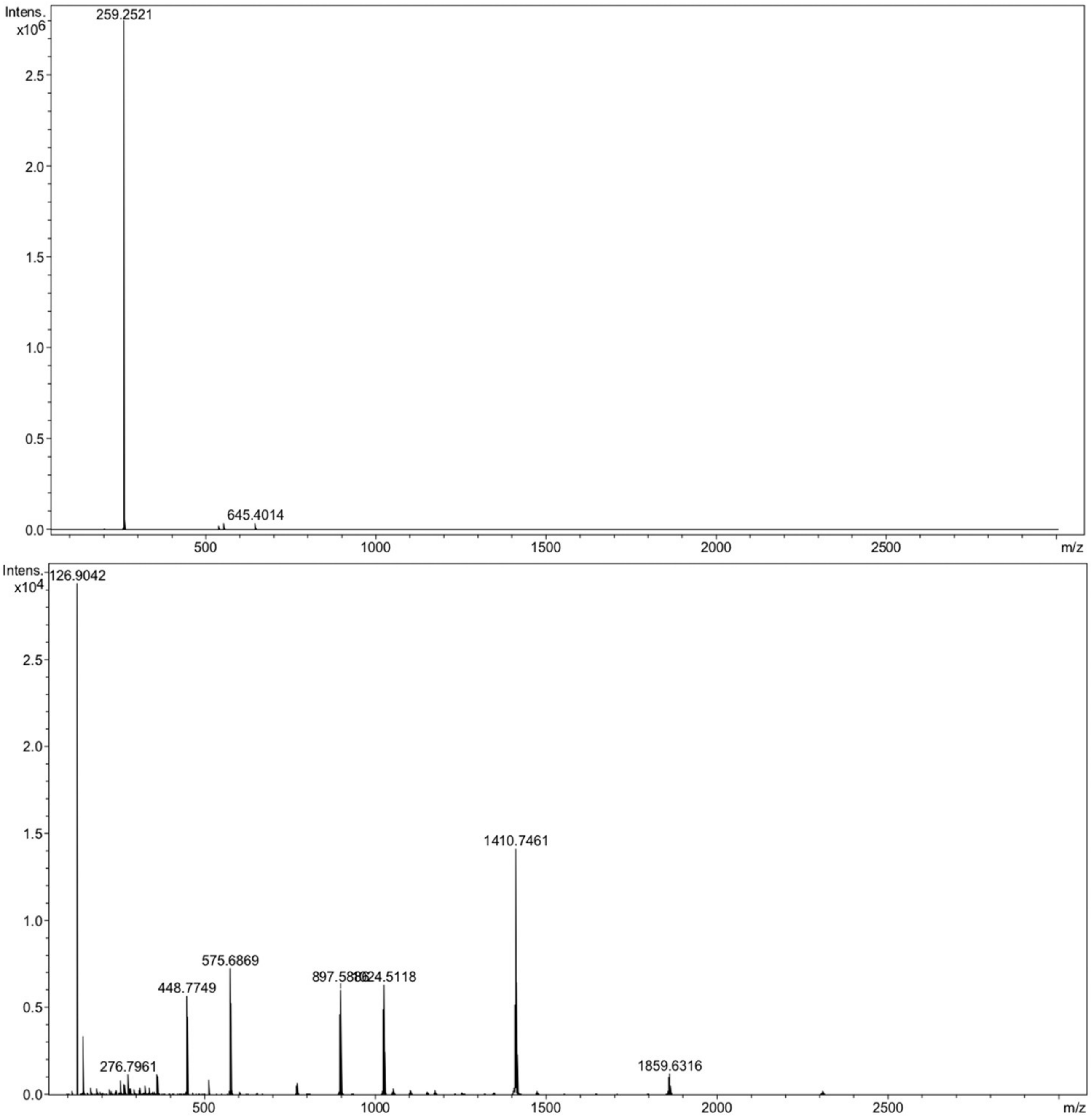

Fig. S33. Mass-spectra of **3**: *top* – HRESI$^+$-MS (calcd. for $[Bu_4P]^+$ 259.2555, found 259.2521); *bottom* – HRESI$^-$-MS (calcd. for $[I]^-$ 126.9045, found 126.9042; calcd. for $[2I^- + Na^+]^-$ 276.7987, found 276.7961; calcd. for $[Pt_2I_6]^{2-}$ 575.6734, found 575.6869; calcd. for $[Pt_2I_5]^-$ 1024.4422, found 1024.5118; calcd. for $[M - Bu_4P^+]^-$ 1410.7021, found 1410.7461).

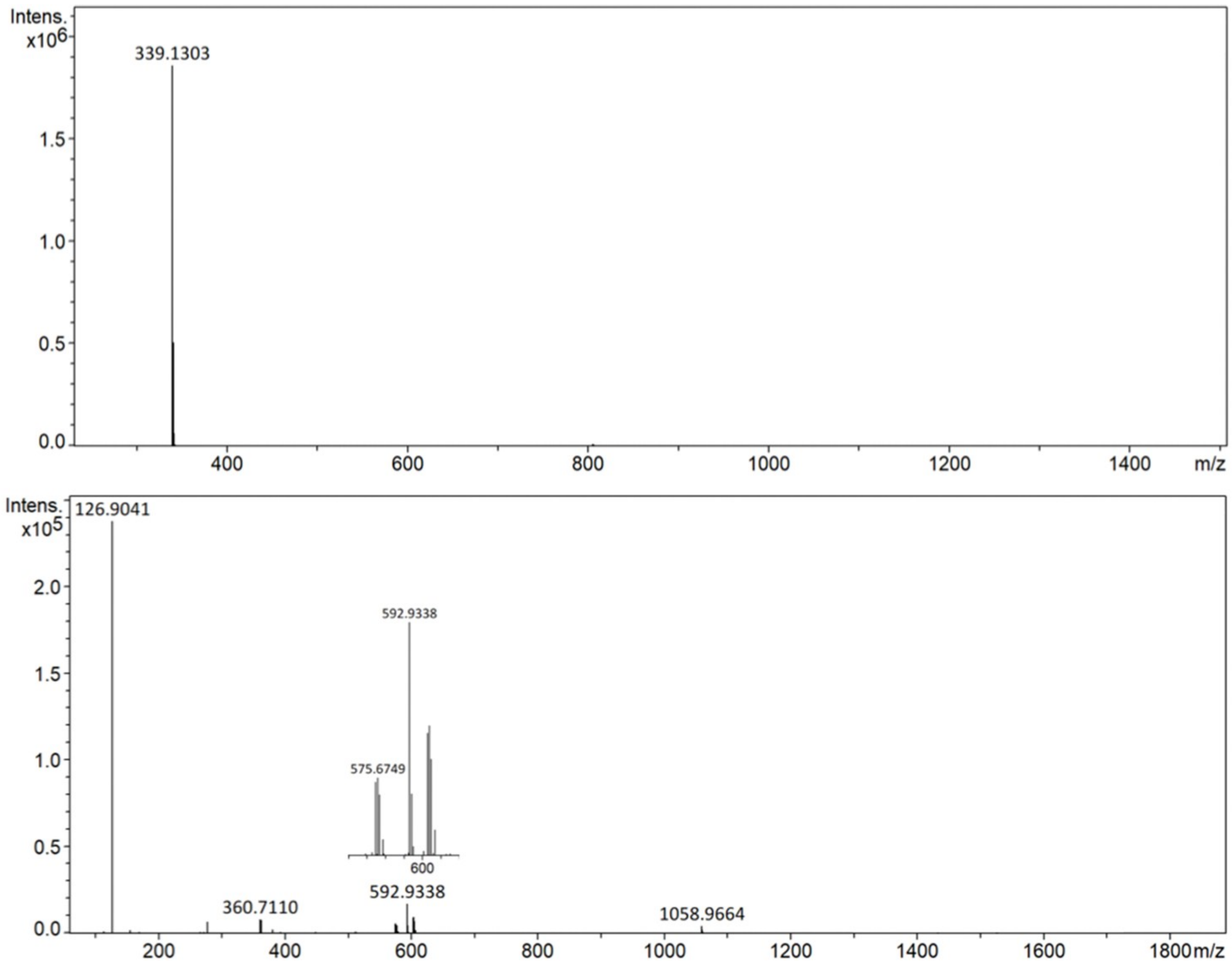

Fig. S34. Mass-spectra of **4**: *top* – HRESI$^+$-MS (calcd. for $[Ph_4P]^+$ 339.1303, found 339.1303); *bottom* – HRESI$^-$-MS (calcd. for $[I]^-$ 126.9045, found 126.9041; calcd. for $[Pt_2I_6]^{2-}$ 575.6734, found 575.6749).

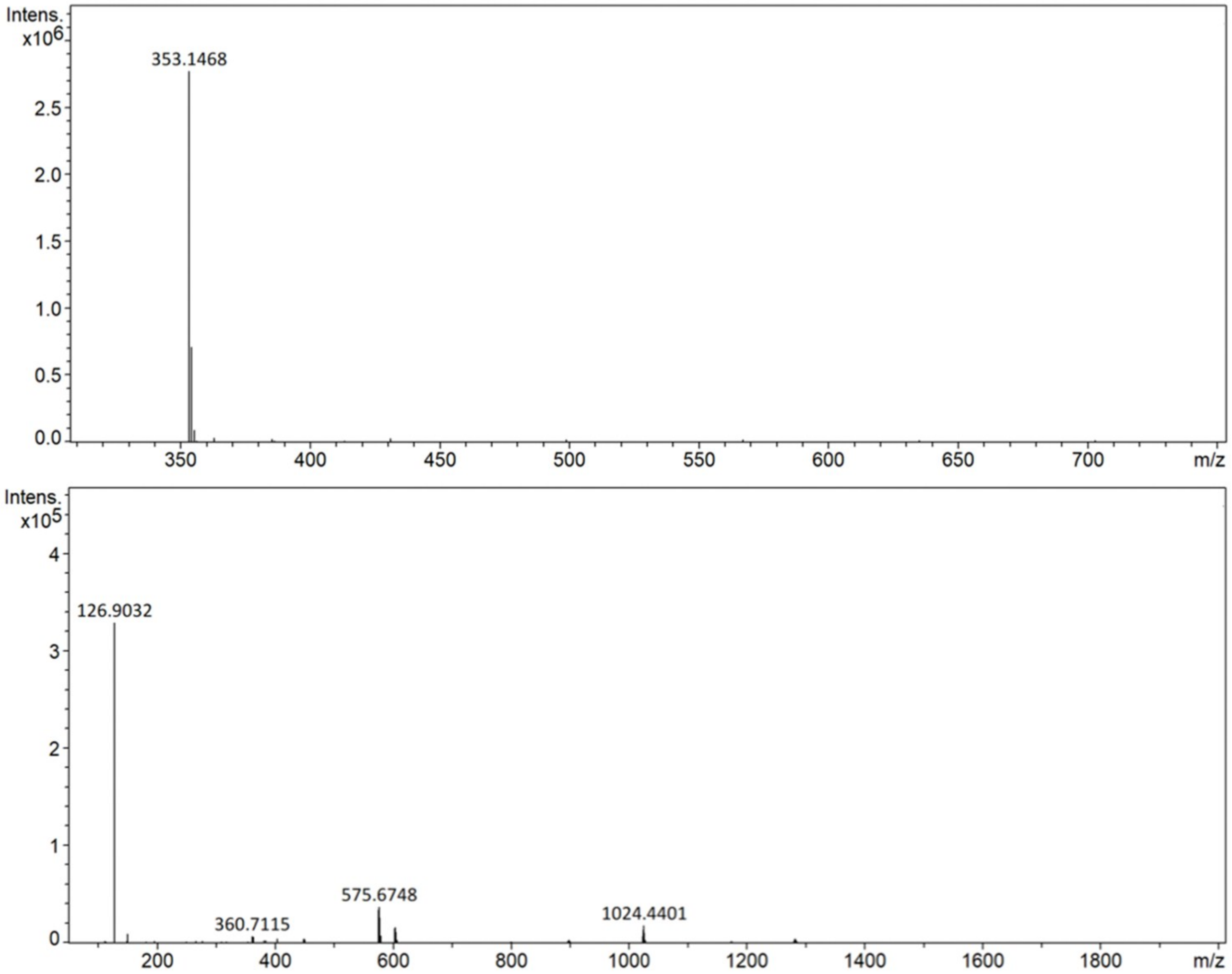

Fig. S35. Mass-spectra of **5**: *top* – HRESI$^+$-MS (calcd. for $[Ph_3PBn]^+$ 353.1459, found 353.1468); *bottom* – HRESI$^-$-MS (calcd. for $[I]^-$ 126.9045, found 126.9032; calcd. for $[Pt_2I_6]^{2-}$ 575.6734, found 575.6748; calcd. for $[Pt_2I_5]^-$ 1024.4422, found 1024.4401).

S4.3 PXRD patterns

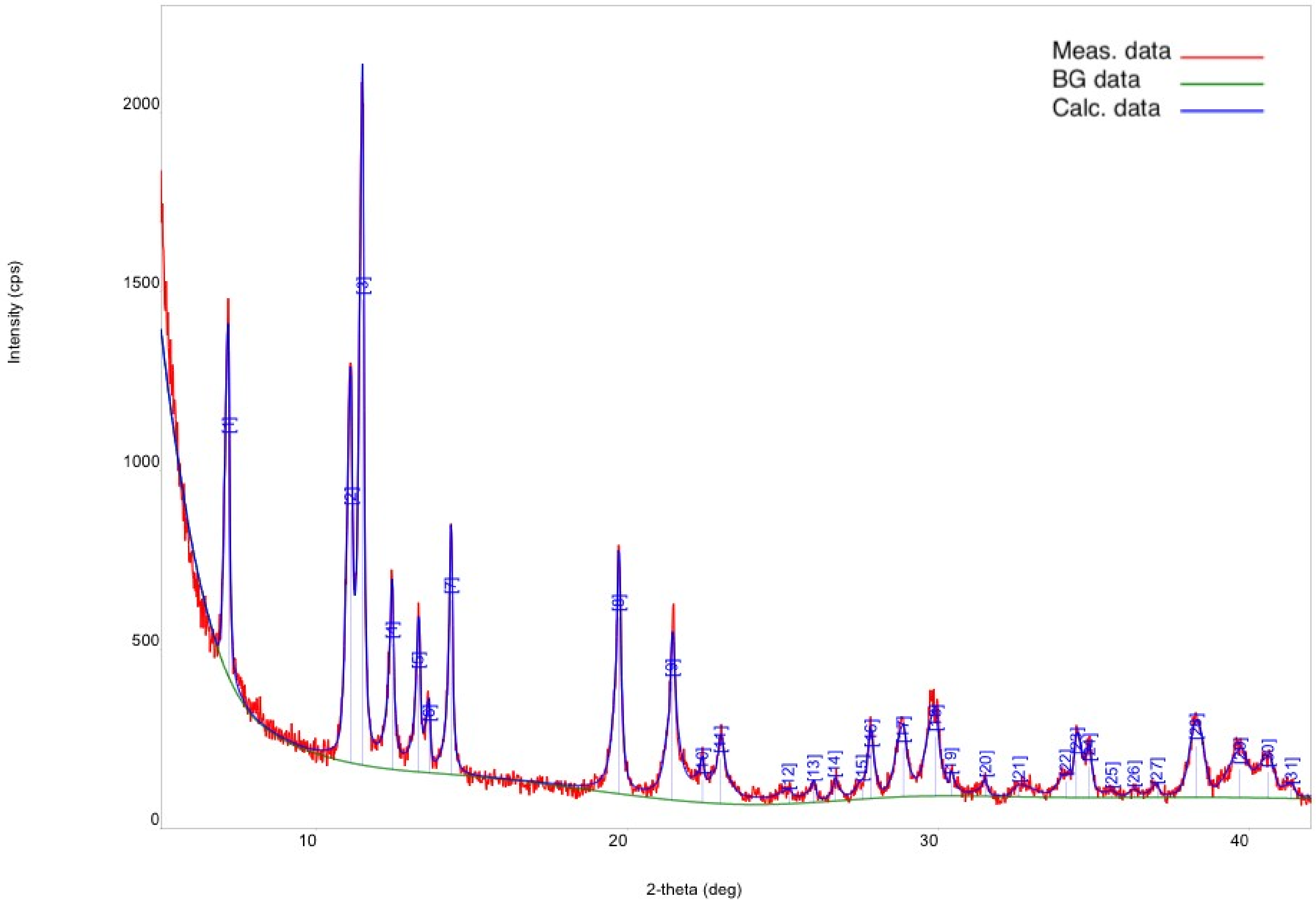

Fig. S36. Comparison of experimental PXRD data (red) with the calculated (blue) for the single-crystal XRD structure of **1**. Hereinafter background data are given in green.

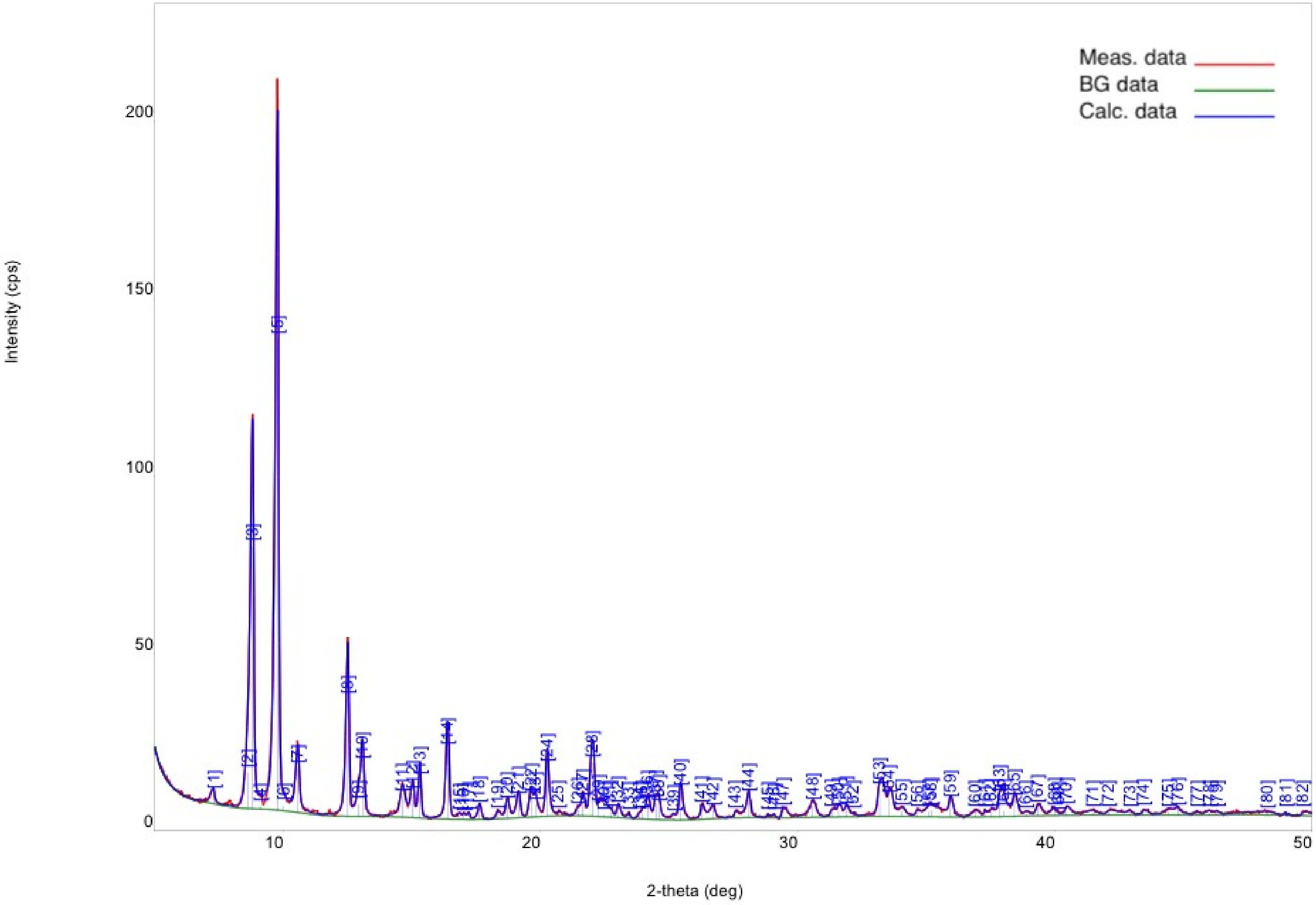

Fig. S37. Comparison of experimental PXRD data (red) with the calculated (blue) for the single-crystal XRD structure of **2**.

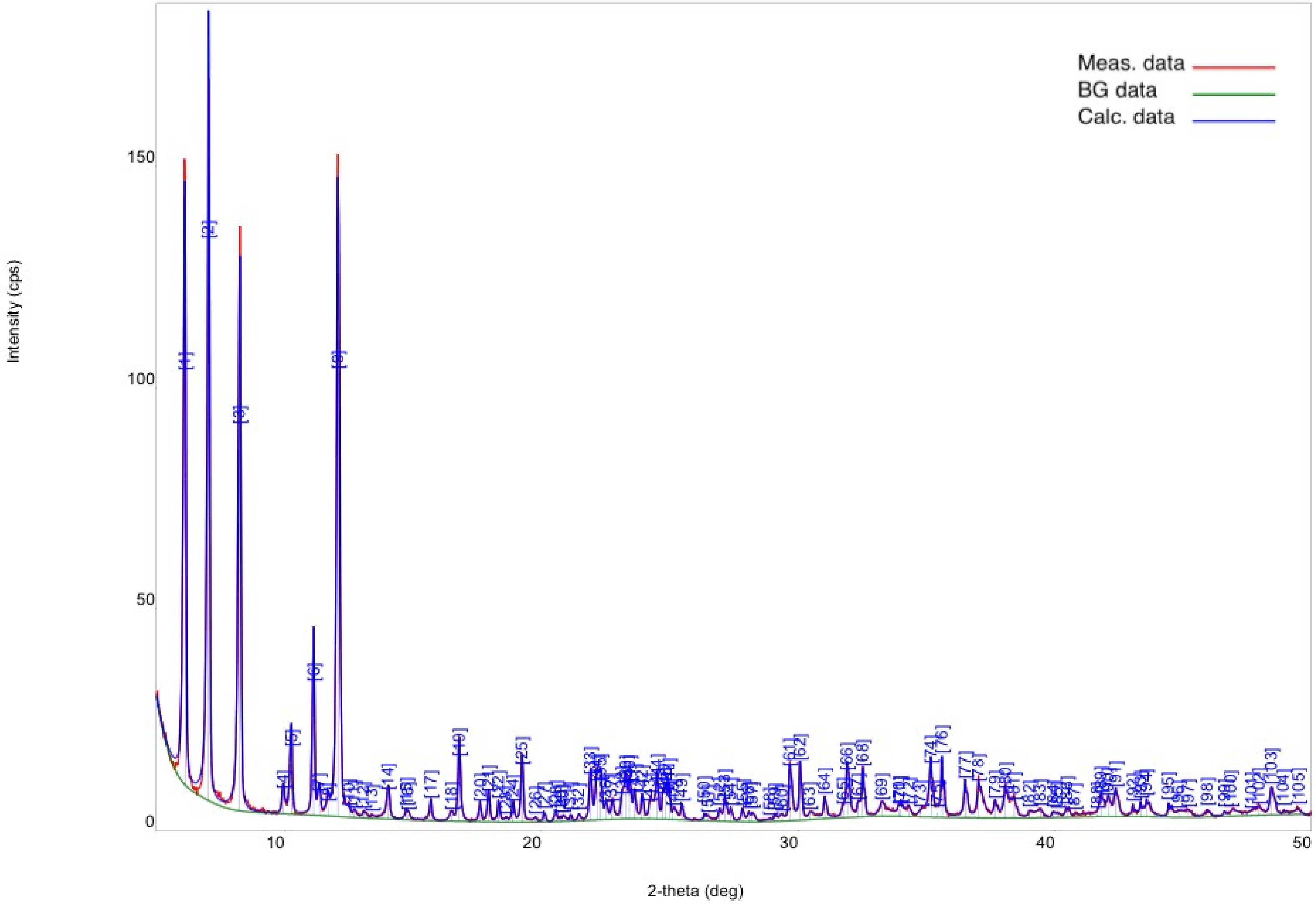

Fig. S38. Comparison of experimental PXRD data (red) with the calculated (blue) for the single-crystal XRD structure of **3**.

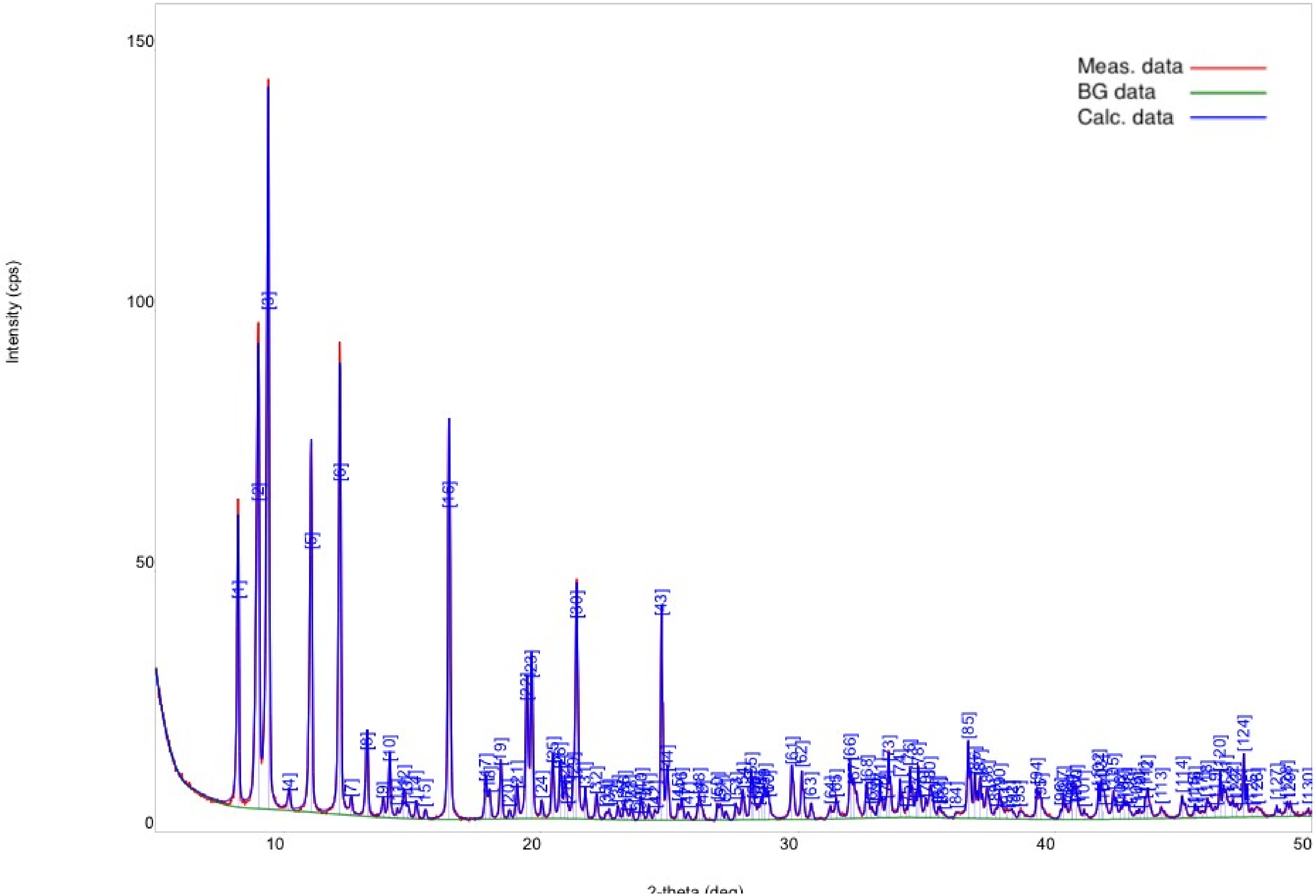

Fig. S39. Comparison of experimental PXRD data (red) with the calculated (blue) for the single-crystal XRD structure of **4**.

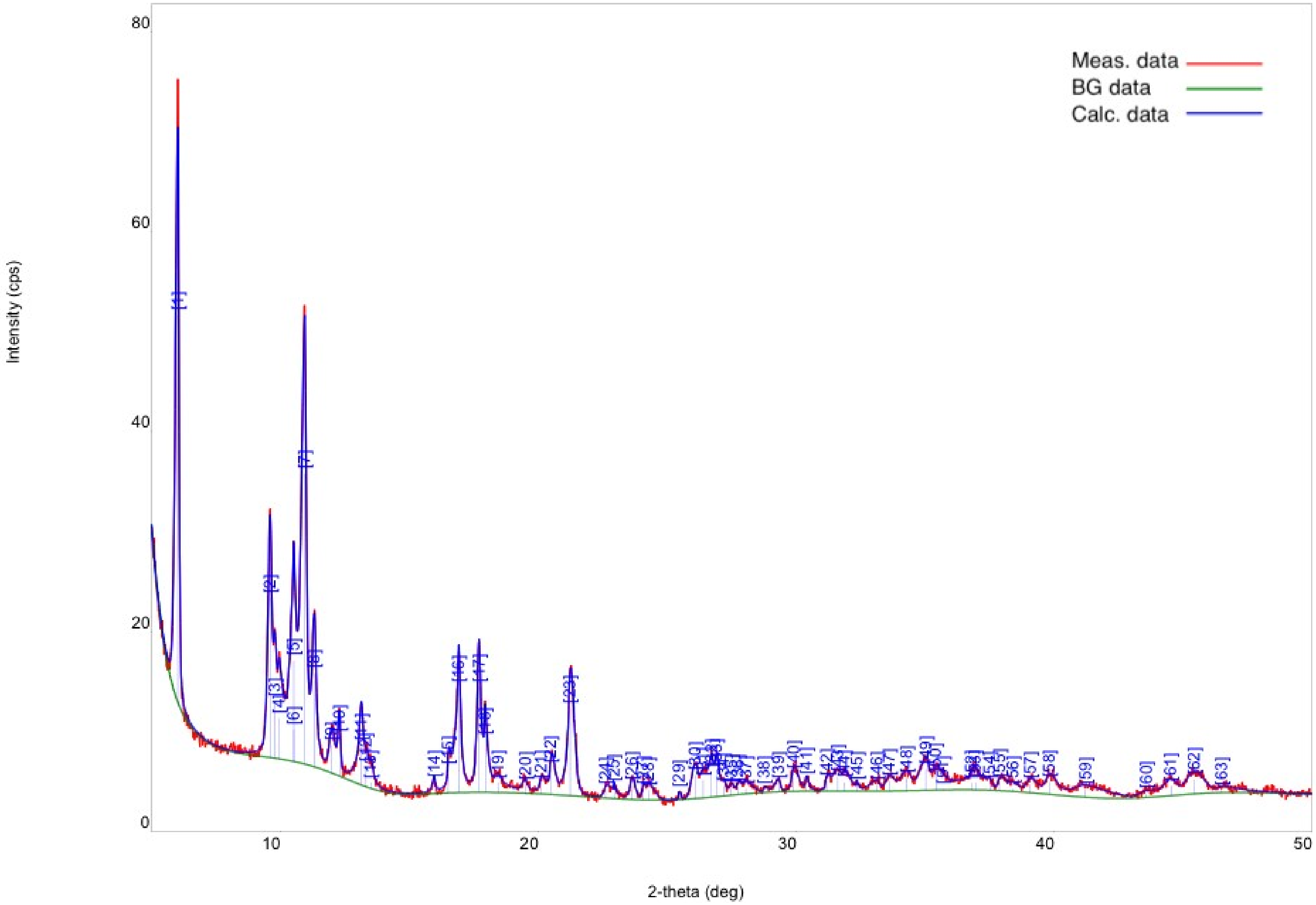

Fig. S40. Comparison of experimental PXRD data (red) with the calculated (blue) for the single-crystal XRD structure of **5**.

S4.4 Raman and FT-IR spectroscopies

The $[\mathrm{Pt_2}(\mu\text{-}\mathrm{I})_2\mathrm{I_4}]^{2-}$ anion belong to D_{2h} point group, which vibrations have the symmetry properties $4A_g + A_u + 3B_{1g} + 2B_{1u} + 2B_{2g} + 3B_{2u} + B_{3g} + 3B_{3u}$; the A_g and B_{1g} vibrations relate to the Raman active in-plane modes.[31–33] The Raman spectra of **1–5** (Fig. S41–S45) show a great similarity between the wavenumbers of the observed bands and those previously calculated for $[\mathrm{Pt_2}(\mu\text{-}\mathrm{I})_2\mathrm{I_4}]^{2-}$,[33] as well as correlate with the Raman data obtained for $[n\mathrm{Pn_4N}]_2[\mathrm{Pt_2}(\mu\text{-}\mathrm{I})_2\mathrm{I_4}]$ in solution (Table S11).[31]

The FT-IR spectra of **1–5** show the bands corresponding to the vibrations of the cations (Fig. S46–S50).

Table S11. Raman data ($\mathrm{cm^{-1}}$) on **1–5**.

		1	**2**	**3**	**4**	**5**	$[n\mathrm{Pn_4N}]_2[\mathrm{Pt_2}(\mu\text{-}\mathrm{I})_2\mathrm{I_4}]$ in $\mathrm{CH_2Cl_2}$ (Ref.[31])	calc. for $[\mathrm{Pt_2}(\mu\text{-}\mathrm{I})_2\mathrm{I_4}]^{2-}$ (Ref.[33])
A_g	**ν_1 Pt–I str.**	192.5 w	191.1 vw, br	192.5 w, br	191.1 vw, br	193.0 vw, br	196	190.1
	ν_2 Pt–I str.	157.7 vs	158.0 s	158.3 vs	157.8 vs	158.7 vs	160	163.9
	ν_3 in-plane def.	92.7 m	90.2 m	91.01m	91.9 m	92.2 m	93	90.5
	ν_4 in-plane def.	64.8 s	62.02 m, br	65.50 m	64.4 w	62.2 m	60	62.3
B_{1g}	**ν_6 Pt–I str.**	192.5 w	191.1 vw, br	192.5 w, br	203.0 vw, br	193.0 vw, br	196	199.0
	ν_7 Pt–I str.	143.2 m	142.8 m	143.2 m	143.2 w	143.8 s	145	145.2
	ν_8 Pt–I str.	–	–	–	83.4 vw, , br	–	–	85.6

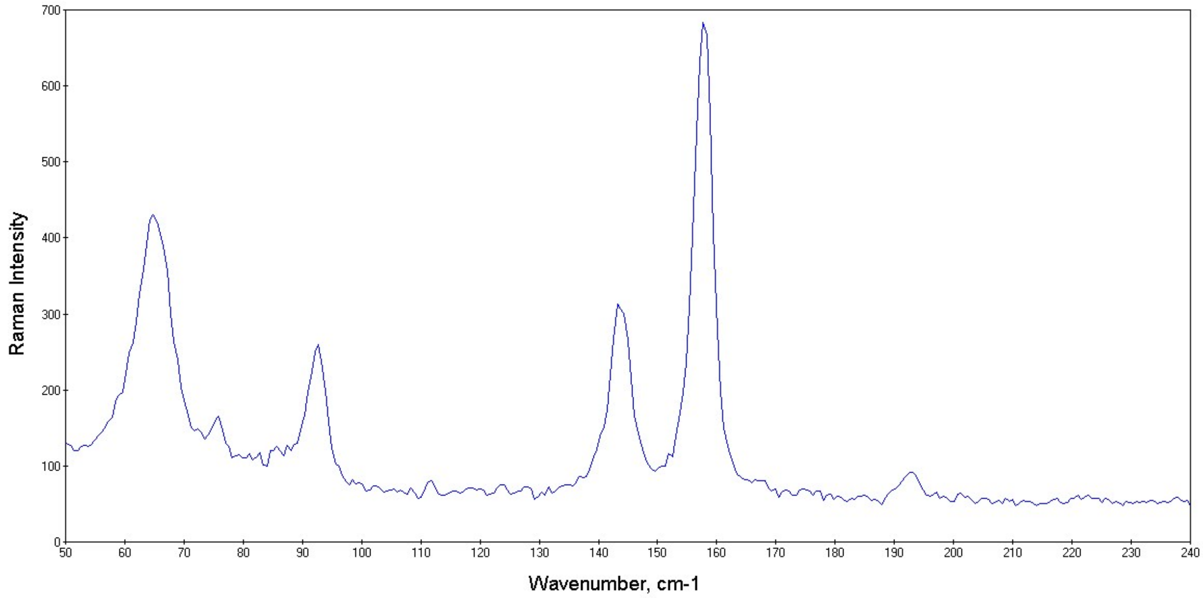

Fig. S41. The Raman spectrum of **1**.

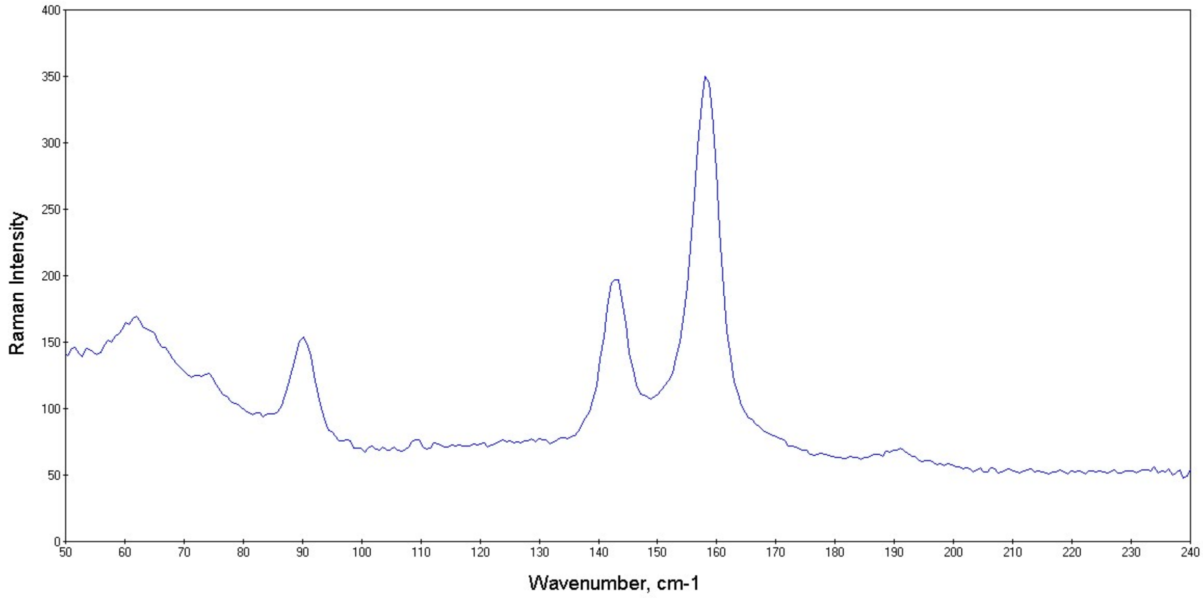

Fig. S42. The Raman spectrum of **2**.

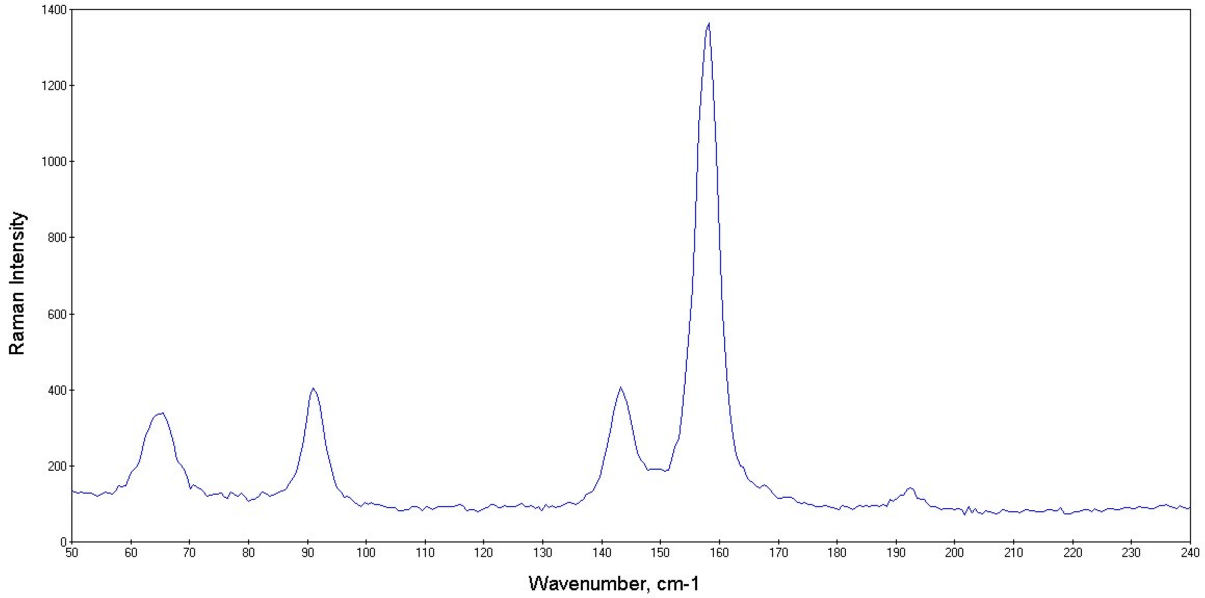

Fig. S43. The Raman spectrum of **3**.

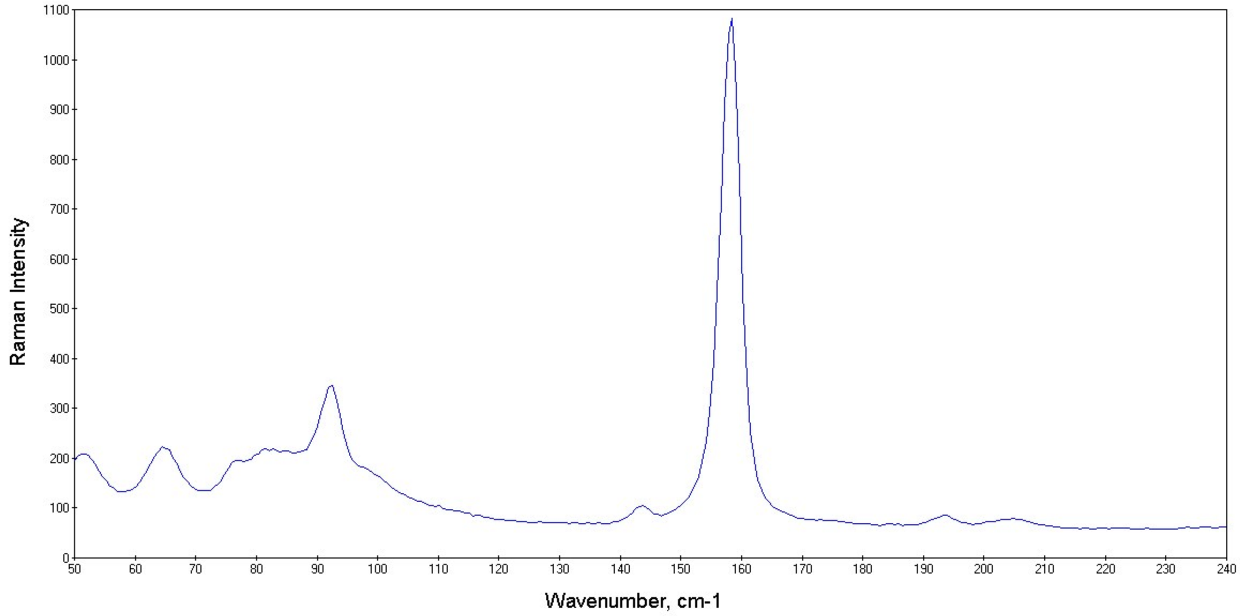

Fig. S44. The Raman spectrum of **4**.

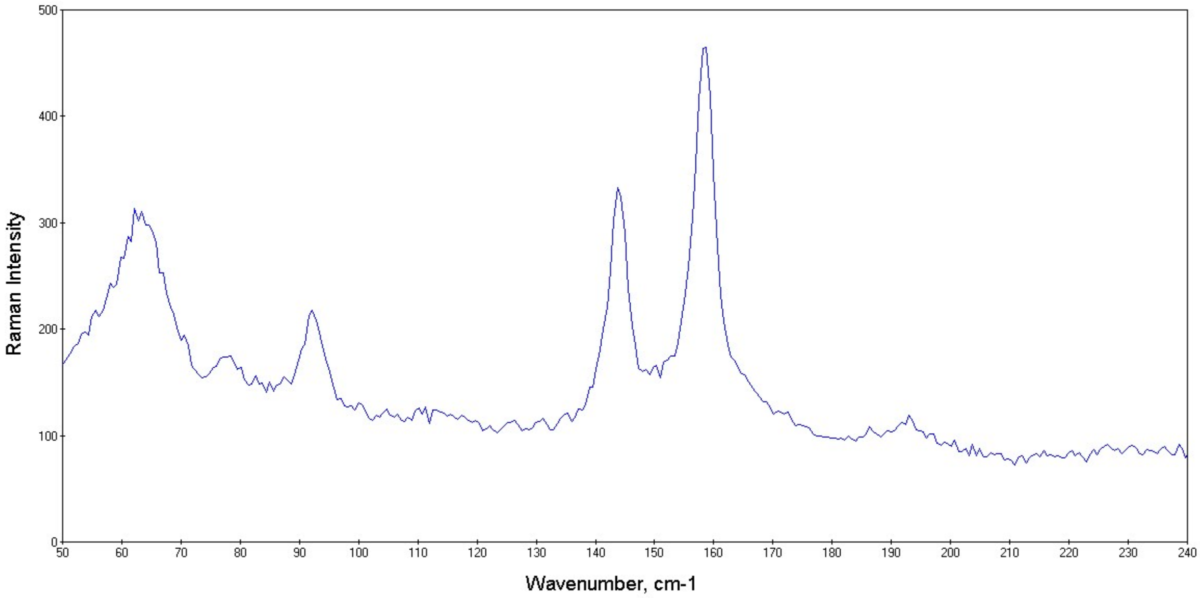

Fig. S45. The Raman spectrum of **5**.

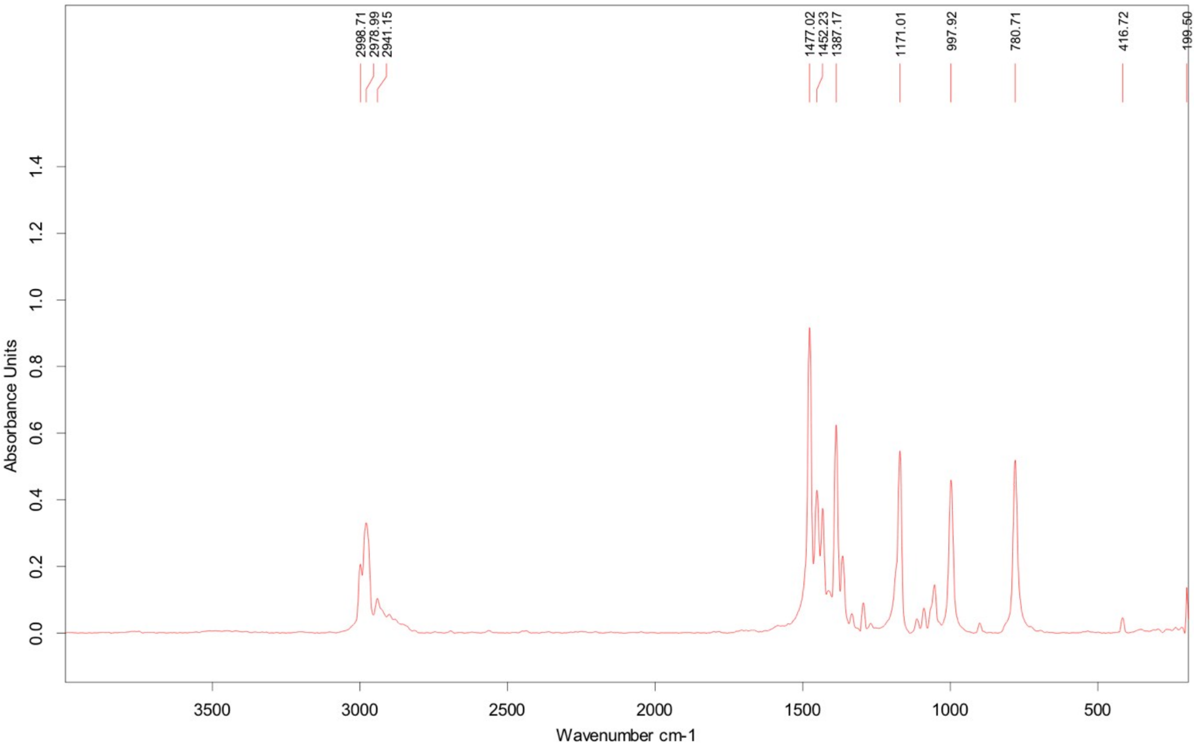

Fig. S46. The FT-IR spectrum of **1**.

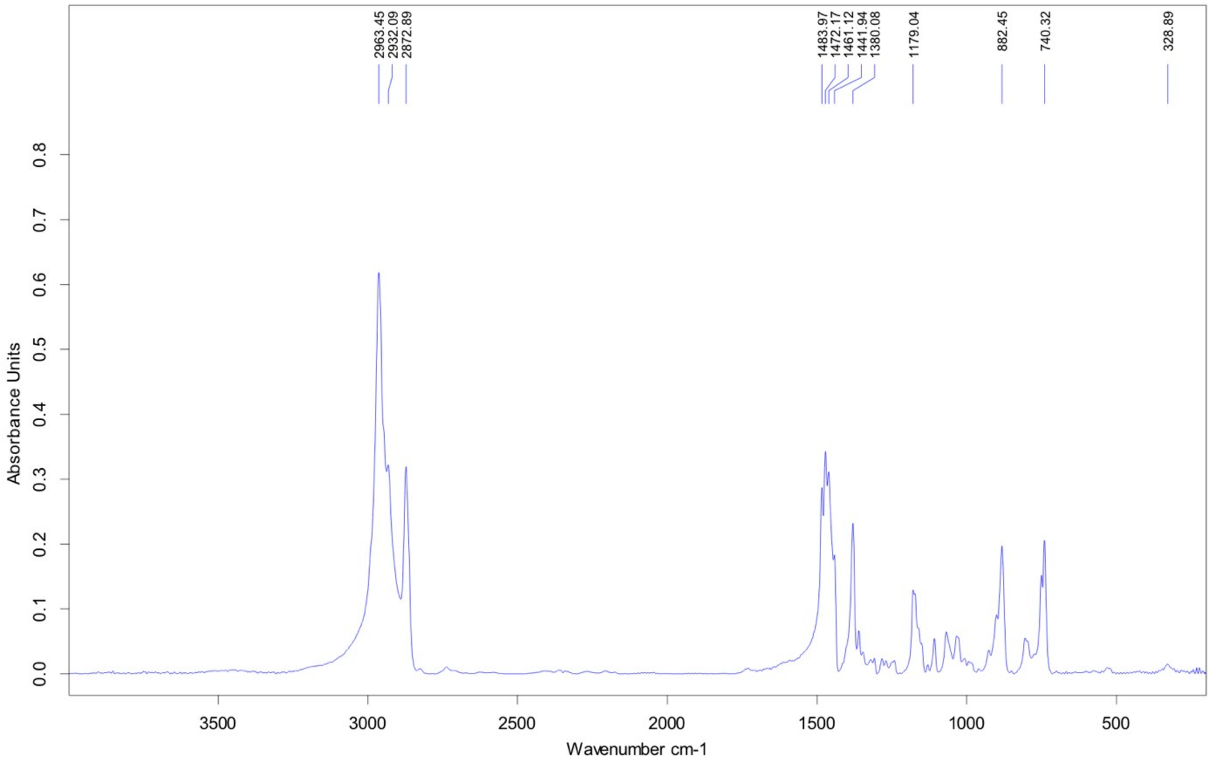

Fig. S47. The FT-IR spectrum of **2**.

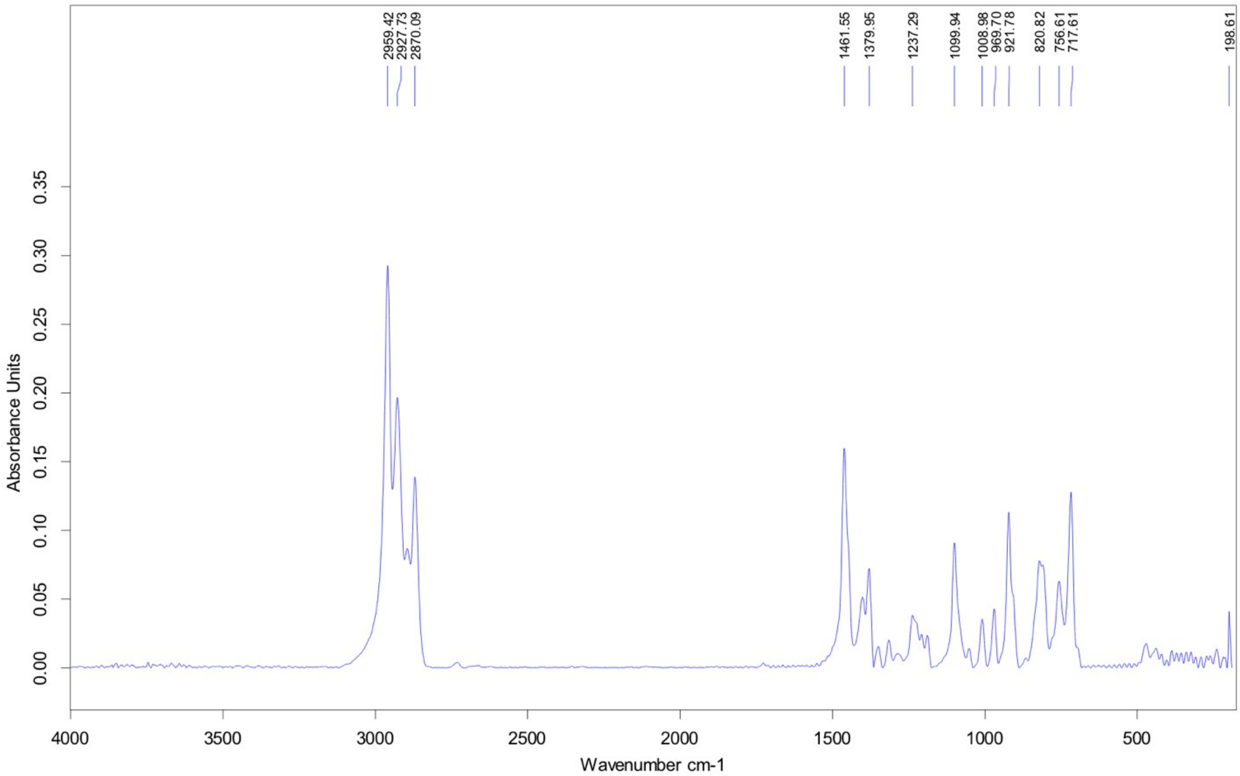

Fig. S48. The FT-IR spectrum of **3**.

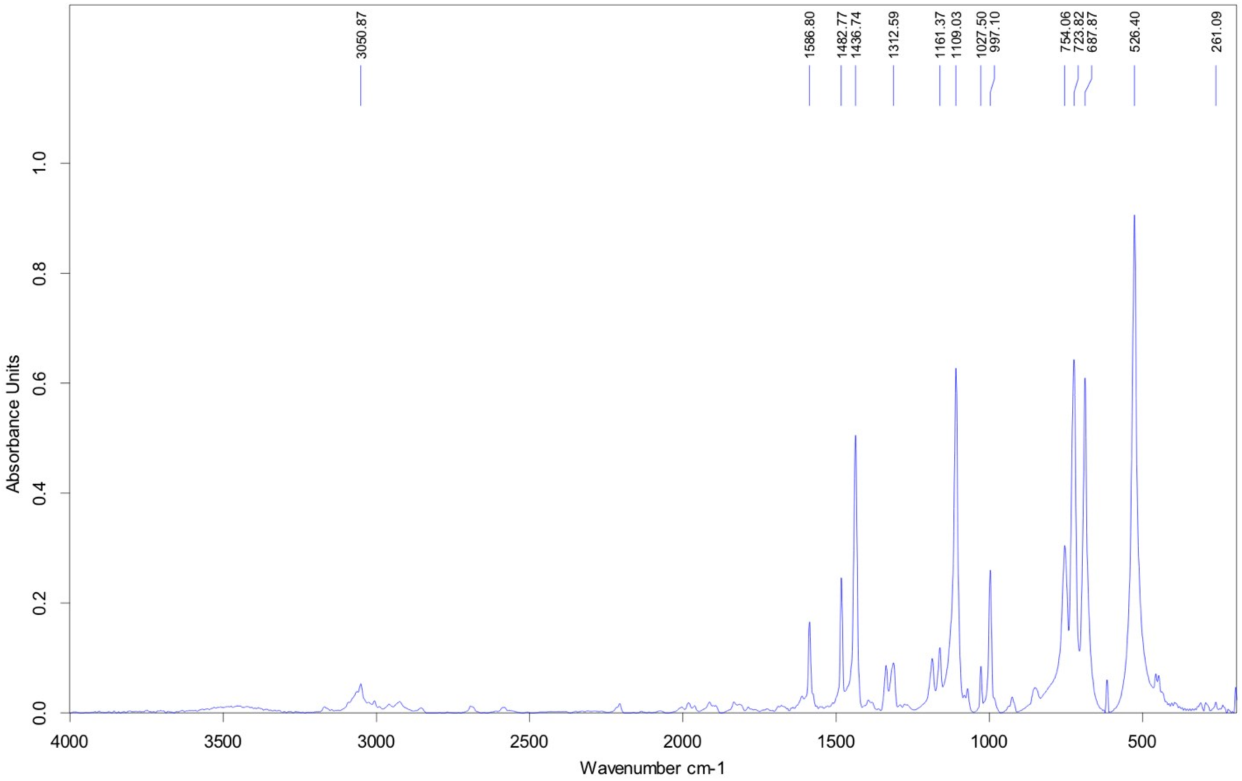

Fig. S49. The FT-IR spectrum of **4**.

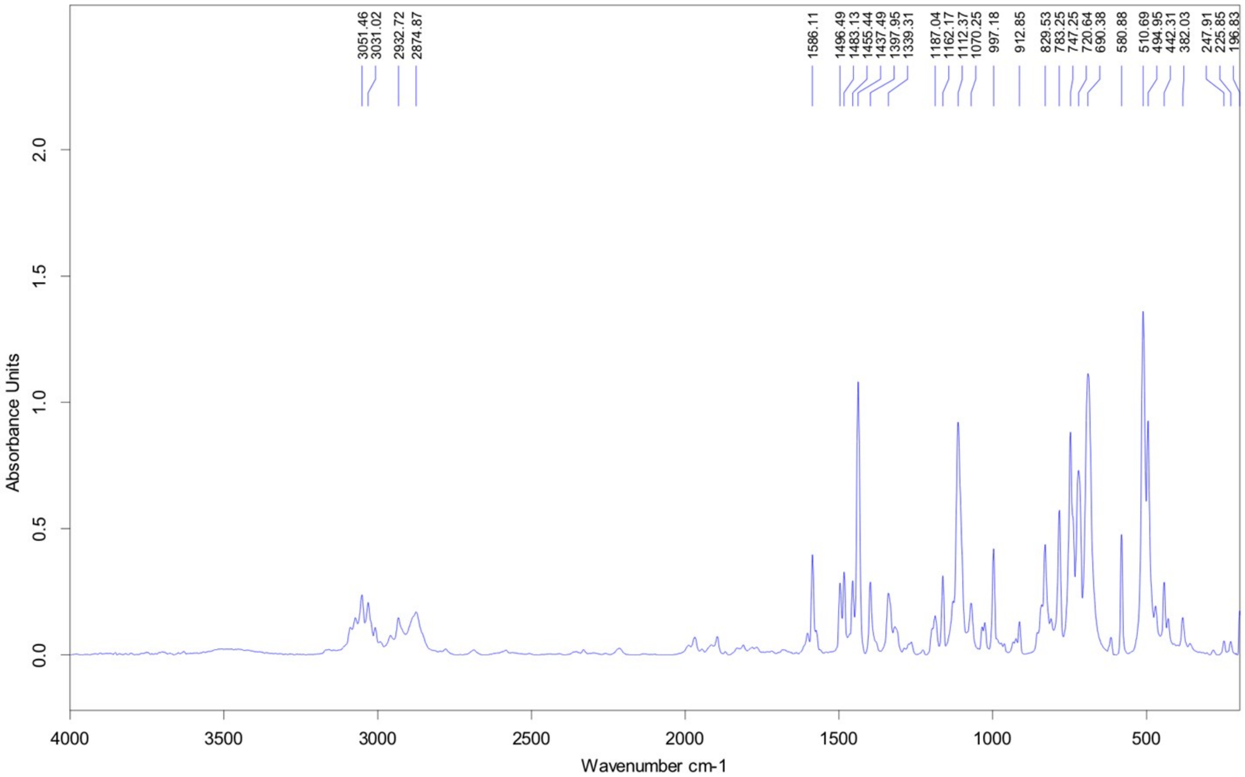

Fig. S50. FT-IR spectrum of **5**.

References

1 C. M. Harris, S. E. Livingstone and N. C. Stephenson, *J. Chem. Soc.*, 1958, 3697–3702.

2 R. J. Dickinson, R. V. (Dick) Parish and B. W. Dale, *J. Chem. Soc. Dalt. Trans.*, 1980, **2**, 895–900.

3 D. M. Adams, P. J. Chandler and R. G. Churchill, *J. Chem. Soc. A Inorganic, Phys. Theor.*, 1967, 1272–1274.

4 R. D. Rogers, H. Isci and W. Roy Mason, *J. Crystallogr. Spectrosc. Res.*, 1984, **14**, 383–392.

5 P. L. Goggin, *J. Chem. Soc. Dalt. Trans.*, 1974, 1483–1486.

6 P. S. Belton, V. C. Ginn, P. F. Kelly and J. D. Woollins, *J. Chem. Soc. Dalt. Trans.*, 1992, 1135.

7 O. F. Wendt and L. I. Elding, *J. Chem. Soc. Dalt. Trans.*, 1997, 4725–4732.

8 P. Day, M. J. Smith and R. J. P. Williams, *J. Chem. Soc. A Inorganic, Phys. Theor.*, 1968, 668–672.

9 G. Brauer, *Handbuch der Präparativen Anorganischen Chemie in drei Bänden - Dritter Band*, Ferdinand Enke Verlag, Stuttgart, Vol. 3., 1981.

10 W. Baechle, H. W. Rotter, G. Thiele and R. J. H. Clark, *Inorganica Chim. Acta*, 1992, **191**, 121–129.

11 G. Thiele, H. W. Rotter and W. Baechle, *Zeitschrift für Anorg. und Allg. Chemie*, 1989, **572**, 55–62.

12 G. Thiele, H. W. Rotter and W. Baechle, *Zeitschrift für Anorg. und Allg. Chemie*, 1994, **620**, 1271–1277.

13 J. Martin-Gil, F. J. Martin-Gil, M. Pérez-Méndez and J. Fayos, *Zeitschrift für Krist.*, 1985, **173**, 179–183.

14 A. Bakalova, R. Petrova, B. Shivachev and H. Varbanov, *J. Coord. Chem.*, 2007, **60**, 1701–1707.

15 O. Novakova, J. Malina, J. Kasparkova, A. Halamikova, V. Bernard, F. Intini, G. Natile and V. Brabec, *Chem. - A Eur. J.*, 2009, **15**, 6211–6221.

16 R. Cini, F. P. Intini, L. Maresca, C. Pacifico and G. Natile, *Eur. J. Inorg. Chem.*, 1998, **1998**, 1305–1312.

17 F. P. Fanizzi, F. P. Intini, L. Maresca, G. Natile and C. Pacifico, *Acta Crystallogr. Sect. C Cryst. Struct. Commun.*, 1999, **55**, 712–714.

18 O. V. Khazipov, M. A. Merzlikina, D. V. Nikytenko, E. V. Khomutova, T. V. Krasnyakova and S. A. Mitchenko, *Russ. J. Gen. Chem.*, 2017, **87**, 128–131.

19 P. Steenwinkel, H. Kooijman, W. J. J. Smeets, A. L. Spek, D. M. Grove and G. van Koten, *Organometallics*, 1998, **17**, 5411–5426.

20 A. A. Eliseeva, D. M. Ivanov, A. S. Novikov and V. Y. Kukushkin, *CrystEngComm*, 2019, **21**, 616–628.

21 D. R. Russell, P. A. Tucker and C. Whittaker, *Acta Crystallogr. Sect. B Struct. Crystallogr. Cryst. Chem.*, 1975, **31**, 2530–2531.

22 S. V. Rosokha and A. Kumar, *J. Mol. Struct.*, 2017, **1138**, 129–135.

23 P. A. Dub, M. Rodriguez-Zubiri, J.-C. Daran, J.-J. Brunet and R. Poli, *Organometallics*, 2009, **28**, 4764–4777.

24 S. V. Rosokha and M. K. Vinakos, *Cryst. Growth Des.*, 2012, **12**, 4149–4156.

25 C. D. Cowman, J. C. Thibeault, R. F. Ziolo and H. B. Gray, *J. Am. Chem. Soc.*, 1976, **98**, 3209–3214.

26 V. Y. Kukushkin, V. M. Tkachuk, I. A. Drol, Z. A. Starikova, B. V. Zhadanov and N. P. Kiseleva, *Russ. J. Gen. Chem.*, 1991, **61**, 51–58.

27 A. Bondi, *J. Phys. Chem.*, 1964, **68**, 441–451.

28 C. Janiak, *J. Chem. Soc. Dalt. Trans.*, 2000, 3885–3896.

29 E. A. Meyer, R. K. Castellano and F. Diederich, *Angew. Chemie Int. Ed.*, 2003, **42**, 1210–1250.

30 C. A. Hunter, K. R. Lawson, J. Perkins and C. J. Urch, *J. Chem. Soc. Perkin Trans. 2*, 2001, 651–669.

31 P. L. Goggin, *J. Chem. Soc., Dalt. Trans.*, 1974, 1483–1486.

32 L. Zhang, H. Wei, Y. Zhang, Z. Guo and L. Zhu, *J. Phys. Chem. A*, 2002, **106**, 3819–3822.

33 P. L. Goggin and J. Mink, *Inorganica Chim. Acta*, 1978, **26**, 119–124.